Available online at www.sciencedirect.com
SCIENCE DIRECT
Geochimica et Cosmochimica Acta 70 (2006) 1677–1694
Geochimica
www.elsevier.com/locate/gca

The role of prokaryotes in subsurface weathering of hydrothermal sediments: A combined geochemical and microbiological investigation

Silke Severmann [a,*], Rachel A. Mills [a], Martin R. Palmer [a], Jon P. Telling [b], Barry Cragg [c], R. John Parkes [c]

[a] *School of Ocean and Earth Science, National Oceanography Centre, University of Southampton, Southampton SO14 3ZH, UK*
[b] *Department of Earth Science, University of Bristol, Queen's Rd., Bristol BS8 1RJ, UK*
[c] *School of Earth, Ocean and Planetary Sciences, Cardiff University, Cardiff CF10 3YE, UK*

Received 27 June 2005; accepted in revised form 13 December 2005

Abstract

A detailed geochemical and microbiological study of a ~2 m sediment core from the inactive *Alvin* mounds within the TAG hydrothermal field was conducted to examine, for the first time, the role of prokaryotes in subsurface weathering of hydrothermal sediments. Results show that there has been substantial post-depositional remobilisation of metal species and diagenetic overprinting of the original high-temperature hydrothermal minerals, and aspects have involved prokaryotic processes. Prokaryotic enumeration demonstrates the presence of a population smaller than the average for deep sea sediments, probably due to the low organic carbon content, but not inhibited by (and hence adapted to) the metal rich environment. There was a small but significant increase in population size associated with the active redox boundary in an upper metal sulphide layer (50–70 cm) around which active metal remobilisation was concentrated (Cu, Au, Cd, Ag, U, Zn and Zn). Hence, subsurface prokaryotes were potentially obtaining energy from metal metabolism in this near surface zone. Close association of numbers of culturable Mn and Fe reducing prokaryotes with subsurface Fe^{2+} and Mn^{2+} pore water profiles suggested active prokaryotic metal reduction at depth in core CD102/43 (to ~175 cm). In addition, a prokaryotic mechanism, which is associated with bacterial sulphate reduction, is invoked to explain the U enrichment on pyrite surfaces and Zn and Pb remobilisation in the upper sediment. Although prokaryotic populations are present throughout this metalliferous sediment, thermodynamic calculations indicated that the inferred low pH of pore waters and the suboxic/anoxic conditions limits the potential energy available from Fe(II) oxidation, which may restrict prokaryotic chemolithotrophic biomass. This suggests that intense prokaryotic Fe oxidation and weathering of seafloor massive sulphide deposits may be restricted to the upper portion of the deposit that is influenced by near neutral pH and oxic seawater unless there is significant subsurface fluid flow.

1. Introduction

Active hydrothermal systems are thought to be ideal for stimulation of microbial activity as there is a ready supply of electron donors and acceptors provided by the metalliferous substrate, pore fluids and low temperature (2–100 °C) hydrothermal fluids that commonly circulate through the periphery of the hydrothermal system and surrounding sediments. In these systems reduced S compounds, Fe(II), Mn(II), H_2 and CH_4 provide additional electron donors, and metal oxides may also be utilised as electron acceptors (Jannasch and Mottl, 1985; McCollom and Shock, 1997; Vargas et al., 1998). This is in contrast to most deep sea sediments where the main electron donor is organic carbon, and its breakdown products from heterotrophic respiration, fermentation and hydrolysis of macromolecular compounds (Jørgensen, 1983).

* Corresponding author. Present address: Department of Earth Sciences, University of California—Riverside, Riverside, CA 92521, USA. Fax: +1 951 827 4324.
E-mail address: silke.severmann@ucr.edu (S. Severmann).

0016-7037/$ - see front matter © 2005 Elsevier Inc. All rights reserved.
doi:10.1016/j.gca.2005.12.008

Large transition metal enrichments occur in sediments surrounding submarine hydrothermal vent systems (Metz et al., 1988; German et al., 1993; Mills et al., 1993), with a significant proportion of the metals being derived from mass wasting and slumping of primary massive sulphides. Sediments close to the vents contain a high proportion of sulphides, and their juxtaposition with oxic seawater produces a substrate that contains sharp redox, pH and temperature gradients. As the hydrothermal mineral assemblages are thermodynamically unstable in oxic seawater, seafloor alteration of hydrothermal deposits occurs (Hannington et al., 1990a,b, 1991).

Recent studies have shown that microbial processes continue to considerable depths (>800 m) in sub-seafloor sediments (Parkes et al., 2000; Schippers et al., 2005), but their in situ metabolic activity and reaction mechanisms are poorly understood (D'Hondt et al., 2002; D'Hondt et al., 2004). Microorganisms affect the direction and rates of chemical transformations (Singer and Stumm, 1970; Kasama and Murakami, 2001) and lower the degree of supersaturation required for mineral precipitation (Fortin et al., 1997; Konhauser, 1998). Consequently, they drive the observed diagenetic reactions occurring with increasing depth in sediments (Froelich et al., 1979) and deviations from equilibrium conditions observed in laboratory incubations (Küsel et al., 2002) and pore fluids (Bottrell et al., 2000).

Within the hydrothermal environment subsurface mixing of fluids and seawater can stimulate growth of large microbial populations (Deming and Baross, 1993; Holden et al., 1998; Parkes et al., 2000; Nercessian et al., 2005). Most microbiological studies at vent sites have focused on chemolithotrophic microorganisms that obtain energy from reduced dissolved chemical species (Jannasch and Mottl, 1985; Wirsen et al., 1986; McCollom and Shock, 1997). By comparison, fewer studies have examined the potential of minerals, such as polymetallic sulphides and metal oxides, as a metabolic substrate (Wirsen et al., 1993; Eberhard et al., 1995; Edwards et al., 2003a; Nercessian et al., 2005). In contrast to dissolved species, hydrothermal minerals provide an energy source for chemolithotrophic growth that may continue to be utilised after active venting has ceased. Subsurface microbial communities in hydrothermal sediments may therefore exist as a continuum of microbial activity from high to low temperatures, throughout the geological life time of the deposit, and drive diagenetic alteration of hydrothermal minerals and including formation of ore bodies (Fallick et al., 2001).

Here, we examine the relationship between subsurface microbial populations and sediment diagenesis at the TAG hydrothermal site to test the hypothesis that microbes play an important role in the subsurface diagenesis of metal-rich hydrothermal sediments.

2. Geological setting: Metalliferous sediments at TAG

The TAG hydrothermal field, located at 26°N on the slow-spreading mid-Atlantic ridge (MAR), hosts one of the largest known sea floor massive sulphide deposits on mid-ocean spreading axis (Humphris et al., 1995). A wide range of active and fossil hydrothermal deposits are found here in an area of 5×5 km between 2400 and 3500 m water depth, including the currently active high-temperature TAG mound, the zone of low temperature venting on the east rift valley wall and two relict massive sulphide deposits *Mir* and *Alvin* (Thompson et al., 1985; Rona et al., 1993). The *Alvin* zone comprises a chain of relict sulphide mounds, which are undergoing oxidation, mass wasting and burial by carbonate sedimentation (Rona et al., 1993; Rona et al., 1998; White et al., 1998). Radiometric dating suggests intermittent hydrothermal activity over at least 75,000 years (Lalou et al., 1995), and warm fluids (22.5 °C) have been observed in the northern *Alvin* zone (Rona et al., 1998; White et al., 1998). Metalliferous sediments in this area represent different styles of venting (high temperature focused or low temperature diffuse) and modes of deposition (mass wasting or plume fall-out) (e.g., Thompson et al., 1985; Metz et al., 1988; German et al., 1993; Mills et al., 1993).

Hydrothermal sediments for this study were collected at 3595 m water depth from the southern periphery of the *Alvin* zone near the relict Southern Mound (core CD102/43; Fig. 1). The mineral assemblages at this site (see core-log in Fig. 2) closely resemble those of sediments that have previously been described for this area and are typical for metalliferous sediments that form in the immediate vicinity of high-temperature hydrothermal vents (Metz et al., 1988; Mills et al., 1993). Previously published data from core CD102/ 43, in particular rare earth element (REE) and $\delta^{18}O$ analyses of clay minerals, support the following stratigraphic interpretation (Severmann et al., 2004): The two sulphide layers are dominated by pyrite, with minor chalcopyrite and sphalerite, consistent with the sediments being derived from mass wasting of a hydrothermal massive sulphide deposit (e.g., Metz et al., 1988). Between emplacement of the first and second sulphide layers there was a period of pelagic sediment deposition, as evidenced by continental $^{87}Sr/^{86}Sr$ signatures in clay phases from the Fe-oxide layer overlying the lower sulphide zone (Severmann et al., 2004). REE distributions indicate that the entire core has interacted with both hydrothermal fluids and seawater to varying extents, with the oxide layers having experienced the greatest degree of seawater interaction (Severmann et al., 2004). Fe-oxysilicates within the oxide layer (70–165 cm) formed dominantly by oxidation and precipitation of dissolved Fe^{2+} from low-temperature fluids rather than by oxidation of sulphides. $\delta^{18}O$ analyses of authigenic minerals (largely nontronite and Fe-oxides) from the intermediate layer suggest that these sediments experienced temperatures of 60–85 °C (Severmann et al., 2004), although the temperature of the sediments was only ~2 °C when the core was recovered. The presence of nontronite indicates that these circulating fluids

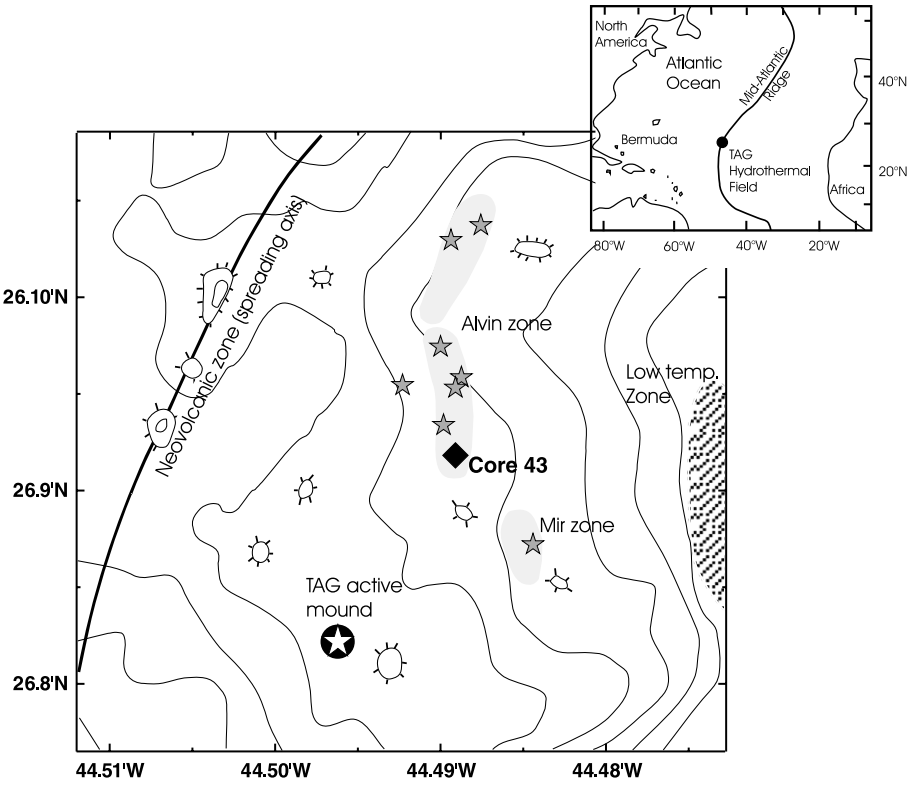

Fig. 1. Map of the TAG area showing active and inactive mounds and the location of core CD102/43. Stars represent chimney features, shading represents sulphide mounds.

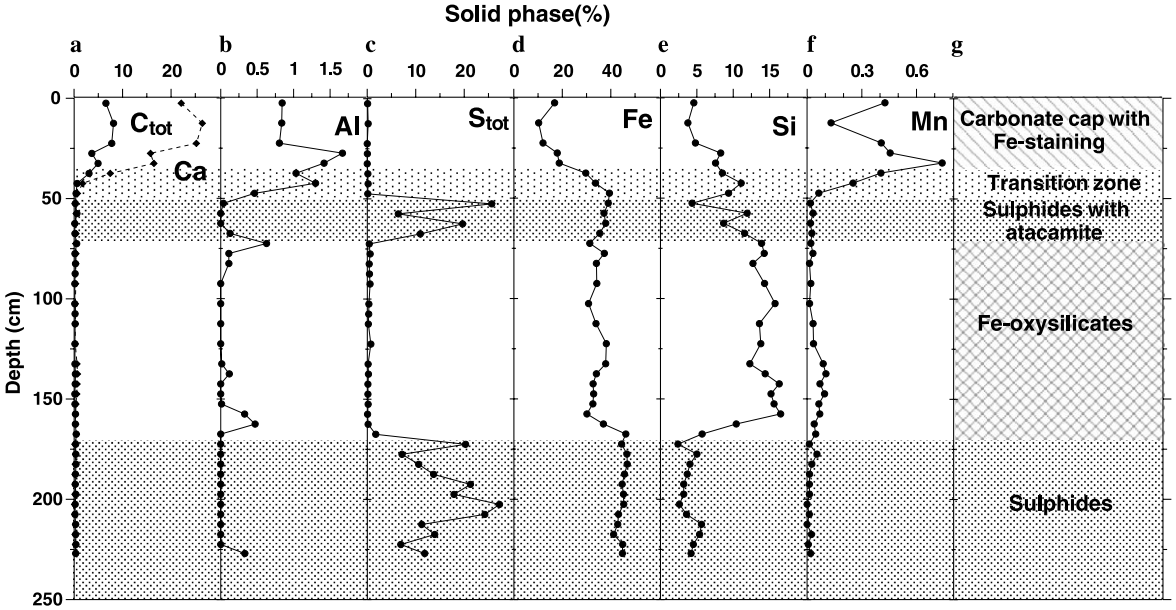

Fig. 2. Down core distribution of (a) Total C ($CaCO_3$ + organic C) and Ca, (b) Al, (c) total S and, (d) Fe, (e) Si, (f) Mn and, (g) simplified core log. Shaded areas in this and all following figures are zones of high concentrations of hydrothermal sulphide minerals.

had low pH (which accounts for the absence of $CaCO_3$ in the intermediate layer) and the environment was suboxic (Malahoff et al., 1982; McMurtry et al., 1983). Following the most recent period of mass wasting, which emplaced the upper metal sulphide layer, a return to pelagic deposition produced the carbonate cap (Fig. 2). The REE composition of the carbonate-rich surface sediments (Severmann et al., 2004) closely resembles those of plume-derived sediments from TAG (German et al., 1993; Mills et al., 1993).

3. Sampling and methods

Several 1–3 m long gravity cores were collected from the inactive '*Alvin*' metalliferous mound in the TAG hydrothermal field during RRS Charles Darwin cruise 102 in 1997 and the core studied here is CD102/43. A background pelagic core (CD102/10) was collected in 3350 m of water depth at 29°23′N, 43°25′W, outside the median valley, to provide a low metal control site for this study. Immediately after sampling, cores were cut into 5 cm depth sections using only sterile (autoclaved) apparatus. During cutting, the surfaces were continually purged with sterile nitrogen and capped immediately to minimise atmospheric exposure. Sectioning was completed within 2 h and any further handling was completed within 12 h in a temperature controlled laboratory at ~4 °C in an O_2-free environment. Alternate depth sections were transferred into a sterile glove bag for microbiological handling and the remaining sections were handled in separate glove bags for geochemical processing. It was not possible to maintain in situ pressure during microbiological processing, but as all depth sections were treated the same, results can still be directly compared. In addition, results from similarly decompressed but even deeper samples have consistently correlated with related geochemical profiles which indicates that results obtained from depressurised samples are environmentally relevant (Parkes et al., 2000).

Pore fluids were extracted by centrifugation and filtration through 0.2 μm filters. Small aliquots of pore water were used for on-board nutrient analysis, including dissolved inorganic silicate and hydrogen-sulphide (colourimetrically, detection limit ~1 μM; Cline, 1969; Koroleff, 1983). Additional aliquots were frozen and stored for subsequent sulphate analysis by ion exchange chromatography. The precision for sulphate analysis is typically better than ±1% (2σ). The remaining pore water was acidified to pH <2 using ultrapure 6 M HCl. Dissolved Fe, Mn, Cu and Cd concentrations were measured on a graphite furnace atomic adsorption spectrometer (using a Pt matrix modifier for Fe and Mn; Sachsenberg et al., 1993). Transition metals were pre-concentrated and purified using a modified version of the micro-extraction technique of Rivera-Duarte and Flegal (1996). Repeat analysis showed that the intra-batch precision was better than ±10% (2σ). U concentrations in the pore fluids were determined by ICP-MS, with an external precision better than ±6% (2σ).

Sediments for geochemical analysis were stored under N_2 and refrigerated. Bulk mineralogy was determined by X-ray diffraction on an automated powder diffractometer using Co-Kα radiation. Dry powder mounts were scanned between 0° and 60° at 1.2° 2θ/min. Si, Al, Fe, Mn, Ca, Cu and Zn sediment concentrations were determined by XRF spectrometry. External precision was ±5–10% for Mn, Cu and Zn (2σ). Accuracy was better than 3% for all elements except Cu and Zn, which were better than 6% (2σ). Au, Ag, Cd, Pb and U were measured by ICP-MS. Accuracy of the analyses was monitored by analysis of standard reference materials (BEN: basalt standard; NOD-P1: international manganese nodule standard, BRR: basalt standard), and was better than ±5% (2σ). Co levels were determined by ICP-AES. Analytical precision was ±5% (2σ). Total carbon, organic carbon and total sulphur were analysed with an elemental analyser calibrated with calcite (C) and acetanilide (S). For organic carbon analyses $CaCO_3$ was removed by acidification with HCl (Nieuwnenhuize et al., 1994).

Samples for SEM analysis were prepared from wet sediments, which were dried at 60 °C and impregnated in resin. Thin sections of the impregnated blocks were mounted on glass slides, polished and carbon coated, before analysis with a JSM 6400 SEM fitted with an Energy Dispersive Spectrometer (EDS) X-ray detector and interfaced with a PGT IMIX image processing system. Elemental compositions were obtained from X-ray single-point analyses, where each point was scanned for relative abundances of selected elements (Fe, S and U) for 30–60 s.

Direct bacterial abundances were quantified in triplicate on 1 cm^3 aliquots of sediment by acridine orange direct count (AODC, Cragg and Parkes, 1993). The fraction of dividing and divided cells (FDDC) was recorded during total cell counts and is expressed as a % thereof (Getliff et al., 1992). FDDC reflects the number of cells that have been or are involved in cell division and is thus a general indicator of the population activity. Dividing cells are two cells of identical morphology attached to each other or a large single cell with an observable invagination; divided cells are two cells of identical morphology in line with a gap between them.

Potential rates of bacterial growth, acetate utilisation and SO_4^{2-} reduction were obtained by incubation of intact syringe subcores (5 cm^3) that had been injected with sterile radioactive tracer ([^{3}H]methyl thymidine, (1,2)[^{14}C]sodium acetate and $^{35}SO_4^{2-}$, respectively). Bacterial growth was assessed by [^{3}H]methyl thymidine incorporation into DNA (Cragg et al., 1992). Potential SO_4^{2-} reduction rates (SRR) were determined by [^{35}S]sulphide formation using an adapted sequential distillation procedure, which also provided concentrations of acid volatile sulphide ($AVS = H_2S + FeS$) (Parkes and Buckingham, 1986). The potential total SRR was calculated from activity measurements, pore water SO_4^{2-} concentration and the sediment porosity. Potential rates of acetate utilisation were determined by the method of Wellsbury and Parkes (1995), whereby $^{14}CO_2$ formation is measured. Potential acetate utilisation rates were calculated from the $^{14}CO_2$ data. The bioavailable acetate pool was determined by the method of King (1991). Radioactivity was measured by liquid scintillation counting (Wallac, UK).

The presence of anaerobic, acetate utilising Fe(III)- and Mn(IV)-reducing microorganisms was determined by the most probable number technique (MPN). This method provides an estimate of specific prokaryotic abundance in a sample by determining the growth of cells or metabolic

end-products in serially descending dilutions of sample that have been incubated in replicate vials of selective growth media. All anaerobic (N_2/CO_2, 80:20) media had either Fe(III) or Mn(IV) as the electron acceptor, acetate as an electron donor, NaCl and $MgCl_2$ at seawater concentrations, resazurin as a redox indicator, trace elements, vitamins and bicarbonate buffer (Telling, 2001). The pH was adjusted to 7.2 and incubation was in the dark at 7 °C. Positive vials were identified by the production of the relevant dissolved reduced metal species.

Thermodynamic calculations were carried out using Geochemist's WorkBench software (Bethke, 1996) and thermodynamic databases SUPCRT92 (Johnson et al., 1992) and EQ3/6 (Wolery, 1992) with recent database updates (http://chess.ensmp.fr/databases.html).

4. Results

4.1. Mineralogy and solid phase compositions

The distribution of major and trace metals in core CD102/43 strongly reflects the mineralogy and stratigraphy outlined above (Fig. 2; Table 1). The sediments contain up to 47% Fe, 4.6% Cu, 0.8% Zn, with the highest metal concentrations associated with the two sulphide layers. The lower portion (165–220 cm) of the core consists predominantly of sulphide (mainly pyrite, with lesser chalcopyrite and sphalerite) with minor amorphous silica. This is overlain (70–165 cm) largely by Fe-oxysilicates plus another thin sulphide layer (50–70 cm) of similar mineralogy to the lower sulphide zone, but more extensively

Table 1
Major and minor element chemistry for TAG metalliferous sediments

Depth (cm)	Si (%)	Al (%)	Fe (%)	Mn (%)	Ca (%)	C_{tot} (%)	C_{org} (%)	S_{tot} (%)	Cu (%)	Zn (%)	Ag (ppm)	Cd (ppm)	Au (ppm)	Pb (ppm)	U (ppm)	Co (ppm)
2.5	4.6	0.8	16.8	0.43	22.1	6.6	0.27	0.1	0.34	0.03	0.0	0.1	0.3	63	4.3	29.5
12.5	3.8	0.8	10.3	0.13	26.4	8.1	0.24	0.2	0.15	0.03	0.2	0.2	0.2	39	2.8	21.3
22.5	4.8	0.8	12.1	0.41	25.2	7.8	0.19	0.0	0.13	0.03	0.0	0.5	0.2	38	3.1	21.4
27.5	8.3	1.7	17.9	0.46	15.8	3.7	0.20	0.0	0.13	0.05	0.8	0.8	0.0	62	4.2	31.8
32.5	7.6	1.4	18.7	0.74	16.5	5.0	0.18	0.0	0.45	0.13	0.1	2.0	0.5	184	8.4	35.4
37.5	8.5	1.0	29.7	0.41	7.5	3.1	0.20	0.1	0.57	0.24	0.1	1.2	0.0	86	5.1	39.2
42.5	11.1	1.3	33.7	0.25	1.8	0.6	0.20	0.2	1.11	0.33	0.1	2.0	1.1	181	8.5	35.3
47.5	9.4	0.5	39.4	0.06	0.7	0.4	0.20	0.1	1.53	0.74	0.3	2.8	1.6	321	9.2	14.9
52.5	4.3	0.0	38.9	0.02	0.2	0.3	0.24	25.7	4.94	0.34	26.9	4.2	4.8	510	27.9	48.1
57.5	11.9	0.0	37.2	0.03	0.4	0.6	0.14	6.4	0.43	0.38	19.4	2.6	0.7	278	13.6	17.0
62.5	8.7	0.0	37.9	0.02	0.2	0.1	0.14	19.7	0.74	0.69	36.2	40.0	0.8	328	15.7	31.0
67.5	11.6	0.1	35.4	0.03	0.4	0.2		10.9	0.35	0.72	3.9	28.8	1.1	310	12.0	20.2
72.5	13.9	0.6	31.3	0.02	0.3	0.5	0.45	0.4	0.06	0.70	1.2	3.4	0.1	198	9.0	8.8
77.5	14.3	0.1	37.3	0.03	0.4	0.2		0.6	0.03	0.40	3.5	0.9	0.2	140	10.2	7.4
82.5	12.7	0.1	34.1	0.01	0.3	0.3	0.15	0.4	0.09	0.45	0.7	0.5	0.4	200	9.8	7.4
92.5	14.3	0.0	34.2	0.02	0.3	0.2	0.16	0.6	0.09	0.35	2.8	2.2	0.2	155	9.9	7.8
102.5	15.7	0.0	30.8	0.01	0.3	0.1	0.28	0.3	0.13	0.27	2.7	1.1	0.1	120	7.1	7.4
107.5											0.8	0.1	0.2	218	8.6	8.7
112.5	13.6	0.0	33.9	0.03	0.2	0.2		0.2	0.14	0.18						
117.5											1.0	0.2	0.4	165	8.7	10.4
122.5	13.8	0.0	38.2	0.03	0.3	0.2	0.15	0.7	0.07	0.15	0.8	0.0	0.3	94	10.2	14.5
127.5											0.5	0.0	0.1	122	8.9	13.2
132.5	12.3	0.0	37.9	0.09	0.6	0.2	0.17	0.2	0.06	0.06	0.0	0.0	0.1	27	11.9	13.7
137.5	14.4	0.1	34.1	0.10.	0.7	0.3	0.14	0.3	0.11	0.05	2.6	0.0	0.0	22	8.7	12.8
142.5	16.3	0.0	32.7	0.07	0.6	0.2		0.2	0.07	0.03	0.0	0.0	0.3	6	11.7	9.8
147.5	15.2	0.0	32.9	0.10	0.6	0.2		0.1	0.08	0.03	0.0	0.0	0.2	27	7.3	12.7
152.5	15.6	0.0	32.6	0.06	0.4	0.2		0.2	0.08	0.03	6.2	0.0	0.2	24	6.6	14.9
157.5	16.5	0.3	30.1	0.07	0.3	0.3	0.21	0.1	0.14	0.04	1.9	0.0	0.2	24	6.1	14.7
162.5	10.4	0.5	37.0	0.04	0.3	0.3	0.22	0.2	0.11	0.04	0.0	0.0	0.5	95	7.7	19.4
167.5	5.7	0.0	46.2	0.05	0.5	0.4	0.29	1.8	1.60	0.12	0.4	0.0	0.0	161	9.7	36.4
172.5	2.4	0.0	44.4	0.01	0.2	0.3	0.24	20.3	4.58	0.21	12.7	6.7	1.9	194	16.4	144.4
177.5	5.0	0.0	46.6	0.05	0.3	0.4	0.24	7.2	1.52	0.12	3.7	0.6	1.4	163	14.6	81.5
182.5	4.0	0.0	46.8	0.03	0.3	0.4		10.6	2.81	0.19	6.5	2.0	1.1	124	16.3	164.6
187.5	3.7	0.0	45.6	0.01	0.2	0.3		13.7	3.76	0.31	10.4	7.3	2.1	190	17.4	161.1
192.5	3.2	0.0	44.7	0.01	0.2	0.2		21.3	4.22	0.24	16.6	22.7	1.4	200	16.4	250.3
197.5	3.2	0.0	45.2	0.01	0.2	0.4	0.27	17.9	4.36	0.59	9.5	4.1	0.9	221	15.2	246.3
202.5	2.6	0.0	45.3	0.0	0.1	0.2		27.3	3.06	0.35	11.7	12.7	1.2	217	18.0	131.5
207.5	3.6	0.0	43.2	0.01	0.1	0.2	0.15	24.2	3.96	0.32	10.9	9.6	0.9	130	18.0	
212.5	5.6	0.0	42.9	0.00	0.3	0.3	1.23	11.2	3.55	0.14	5.4	2.1	0.7	113	15.1	295.3
217.5	5.4	0.0	41.2	0.2	0.2	0.3	0.25	13.9	6.00	0.15	8.6	2.9	1.0	116	15.8	445.7
222.5	4.5	0.0	44.9	0.01	0.3	0.4		6.9	4.26	0.13	4.7	1.3	1.4	155	14.2	201.5
227	4.2	0.3	44.8	0.02	0.3	0.3		11.8	2.57	0.12	5.3	7.0	1.3	156	13.8	104.3

oxidised and recrystallised. The upper 35 cm of the core consists of carbonate ooze that contains 10.3–18.7% Fe. Separating the carbonate cap and the upper sulphide layer is a transition zone which has elevated Fe (29.7–39.4%) and trace element contents. Fe concentrations are high throughout the core (Fig. 2d), whereas Mn is concentrated in the carbonate cap and the transition zone with a minor secondary enrichment in the lower part of the main Fe-oxysilicate zone (Fig. 2f).

Solid phase Cu, Au, Cd, Ag and Co peaks are mainly confined to the sulphide layers (Figs. 6a–e; Table 1). In contrast, elevated Zn and Pb concentrations are present throughout the core, but are particularly enhanced in the two sulphide layers (Figs. 6f–g; Table 1). The U depth distribution is more varied with peaks in both sulphide layers (Fig. 6h; Table 1).

Organic carbon levels are low throughout the core (0.14–0.45%; Table 1). The highest organic carbon contents occur at the base of the upper sulphide layer. AVS concentrations were low throughout the core (<1 mmol/cm^{3}sediment).

The background core consists dominantly of carbonate ooze, with REE compositions that are typical for North Atlantic pelagic background sediments (Severmann et al., 2004).

4.2. Pore water compositions

The average pore fluid SO_4^{2-} concentration (29.0 ± 3 mM) is within measurement error of bottom seawater (28 mM), but elevated SO_4^{2-} concentrations occur in the carbonate cap (33.3 mM) and the lower sulphide layer (32.1 mM) (Fig. 3a; Table 2). Pore fluid Ca levels are within measurement error of seawater values throughout the core (data not shown). Pore water sulphide concentrations are below detection limit (<1 μM) throughout the core.

All pore fluid Fe and Mn is inferred to be present as ferrous and manganous phases respectively. Dissolved Fe^{2+} and Mn^{2+} levels are low in the carbonate cap and transition zone, increase within the upper sulphide layer and remain high throughout the rest of the core. Dissolved Mn^{2+} shows a sharp increase at 52.5 cm from levels below detection limit to 2–4 μM at depth (Fig. 3c; Table 2). Pore water Fe^{2+} increases more gradually, and the highest levels (93 μM) occur in the lower sulphide layer, compared to 33 μM at the base of the upper sulphide layer (Fig. 3b; Table 2).

Pore water profiles of Cu and Cd exhibit maxima within the upper sulphide layer, or in the intermediate layer, while concentrations in the lower sulphide layer are low or below the detection limit (Figs. 6a and c; Table 2). Dissolved U concentrations range between 5 and 13 nM, but no distinct peaks are observed (Fig. 6h; Table 2). Maximum concentrations in the intermediate layer are still lower than typical seawater levels (14 nM; Chen et al., 1986).

Dissolved metal concentrations were mostly below detection limit in the background core CD102/10, and sulphate concentrations were within error of typical seawater values.

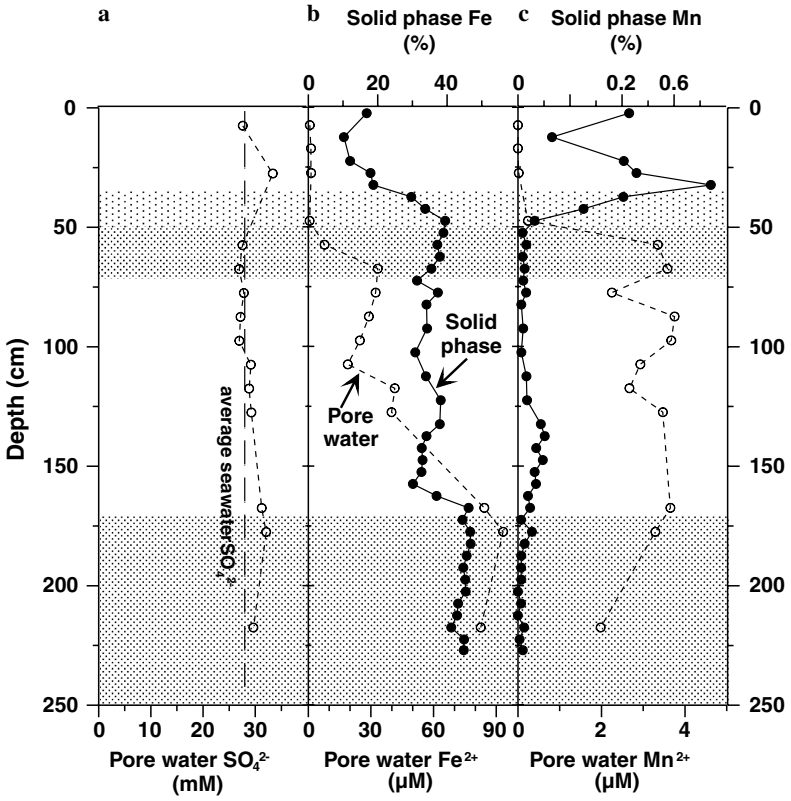

Fig. 3. Down core distribution of (a) SO_4 (dashed lines show ambient seawater values), (b) solid and pore fluid Fe and, (c) solid and pore fluid Mn content.

Table 2
Porewater elemental composition for TAG metalliferous sediments

Sample ID	Depth (cm)	Mn (μM)	Fe (μM)	Cu (μM)	Cd (μM)	U (nM)	SO_4^{2-} (mM)
2	7.5	0.0	0.8	0.0	0.0	10.4	27.6
4	17.2	0.0	1.3	0.0	0.0	9.2	—
6	27.5	0.0	1.4	0.0	0.0	—	33.3
10	47.5	0.2	0.6	1.0	0.0	11.1	—
12	57.5	3.4	7.8	12.1	0.0	10.3	27.6
14	67.5	3.6	33.3	1.1	1.0	10.2	26.9
16	77.5	2.3	32.3	1.9	0.1	12.9	27.8
18	87.5	3.8	29.0	4.6	0.1	12.1	27.2
20	97.5	3.7	24.7	0.3	0.1	12.3	26.9
22	107.5	2.9	18.9	0.7	0.0	8.8	29.2
24	117.5	2.7	41.4	0.8	0.0	10.2	28.8
26	127.5	3.5	39.9	0.7	0.0	7.9	29.3
34	167.5	3.7	84.3	0.0	0.0	—	31.2
36	177.5	3.3	93.3	0.0	0.0	6.0	32.1
44	217.5	2.0	82.6	0.0	0.0	5.0	29.6
Average seawater						14	28

4.3. Prokaryotic abundances and activities

Prokaryotic abundances are low relative to most other deep sediment sites, including other open ocean sites (Fig. 4a), but they are similar to numbers in the nearby background core CD102/10. One-way analysis of variance on microbial population data between 33 and 93 cm depth, across the upper sulphide layer, indicated a significant difference ($F = 23.1$; df = 6,14; $P < 0.001$). An a priori comparison of means test between the data within the sulphide layer and a combination of that both above and below the zone was also highly significant ($F = 68.3$; df = 1,14; $P < 0.001$), with the prokaryotic populations within the sulphide layer being approximately double those on either side. There is, however, no significant difference in the FDDC between the sulphide layer and the surrounding sediment (Fig. 4b).

Many prokaryotes incorporate exogenous thymidine into newly synthesised DNA, the production of which is tightly coupled to cell division and hence carbon produc-

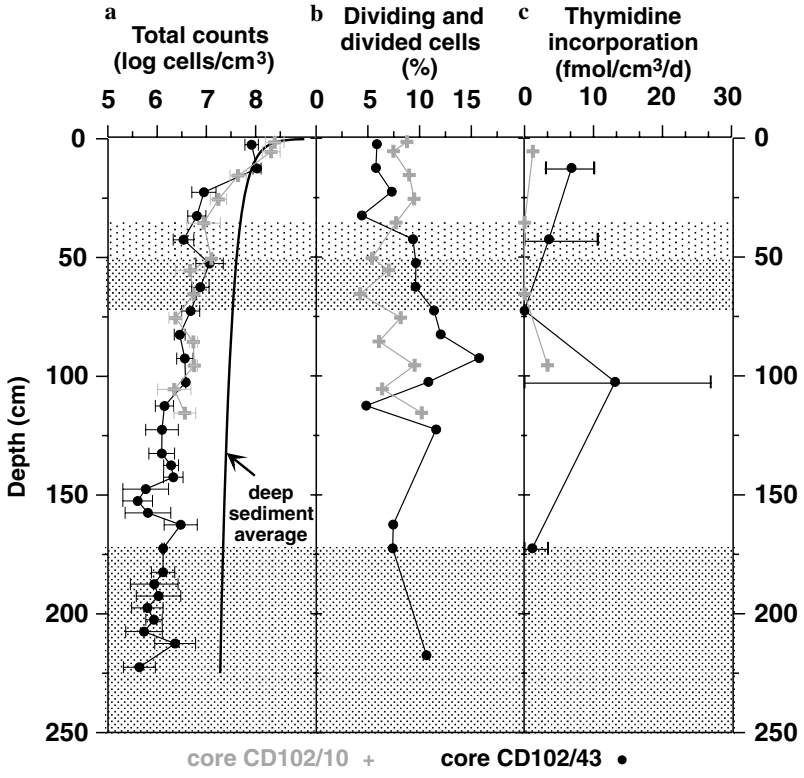

Fig. 4. Down core distribution of (a) total cell counts for core CD102/43 (filled circles) and background core (CD102/10; grey crosses), solid line shows average trend for non-hydrothermal deep sea sediments (regression based on data from ODP Legs 135, 138, 146, 180, 185, 190 and 201) (b) % frequency of dividing and divided cells (FDDC) and (c) thymidine incorporation.

tion and growth. Some prokaryotes, however, are not capable of using exogenous thymidine but will synthesise their own. These include most notably many chemolitho-autotrophic and sulphate-reducing bacteria (Wellsbury et al., 1993). Consequently, the thymidine incorporation method will underestimate total prokaryotic production and productivity estimates in core CD102/43 are minimum values. Thymidine incorporation rates decreased from the surface to the base of the upper sulphide layer, where no significant growth was detected (Fig. 4c). The highest incorporation rates (13 fmol/cm^3/d) were observed in the Fe-oxysilicate zone, and were significantly higher than those in the background core CD102/10 (max rate 3 fmol/cm^3/d). A second but cruder measure of growth activity is the number of dividing and divided cells (Table 6.2, Fig. 4b). No decrease was observed in the surface layer of core CD102/43, but similar to the thymidine incorporation, the FDDC was found to be highest in the intermediate layer, where it reached up to 15% (Fig. 4b). Except for the carbonate cap, FDDC in core CD102/43 tended to be higher than in the background core (CD102/10), particularly in the transition zone, upper sulphide layer and the upper part of the Fe-oxysilicate zone.

Acetate is an intermediate in the anaerobic degradation of organic matter, and acetate oxidation (Fig. 5e) and pore water acetate concentrations (Fig. 5d) have peaks in the transition zone and lower carbonate cap, respectively, broadly coinciding with the maximum rate of SO_4^{2-} reduction (Fig. 5c). Significant populations of Fe and Mn reducers (Figs. 5a and b, up to ca 10^2/cm^3) were present in the lower portions of core CD102/43, and other cores in the same area.

5. Discussion

5.1. Sediment redox conditions

Redox conditions in marine sediments are generally a function of organic carbon decomposition (Froelich et al., 1979), where the intensity of diagenetic remineralization is typically correlated with the intensity of organic carbon respiration (e.g., Thomson et al., 1987; Shaw et al., 1990; Thomson et al., 1998). Organic carbon contents in the sulphidic sediments from the *Alvin* zone are low and similar to levels typical for deep sea sediments (Heath et al., 1977; Emerson, 1985), yet pore water metal concentrations indicate that significant mobilisation is taking place (Figs. 3 and 6). The cause of elevated dissolved metal concentrations in metalliferous sediments at TAG may be reaction between hydrothermal minerals with oxygenated seawater (possibly catalysed by microorganisms), or they may be the result of metal-enriched, low-temperature, fluids percolating through the sediment.

The bulk of the Fe-oxide and nontronite in the intermediate layer was precipitated from low-temperature fluids, as evidenced by the $\delta^{18}O$ composition of these minerals (Severmann et al., 2004). The timing of the nontronite formation is not known, but given the current absence of low temperature venting at this site, it is likely that extensive replacement of pelagic sediments with Fe-oxysilicates

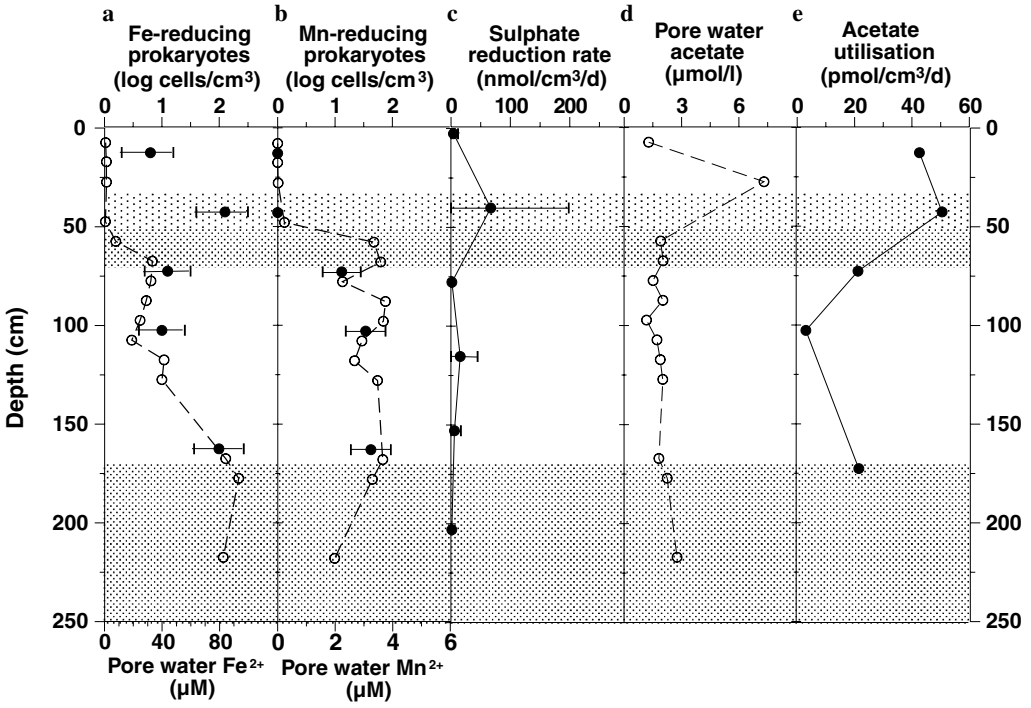

Fig. 5. Down core distribution (a) pore fluid Fe (open circles) and MPN estimates of Fe reducers (filled circles), (b) pore fluid Mn (open circles) and MPN estimates of Mn reducers (filled circles), (c) SRR, (d) pore water acetate and (e) acetate utilisation in core CD102/43.

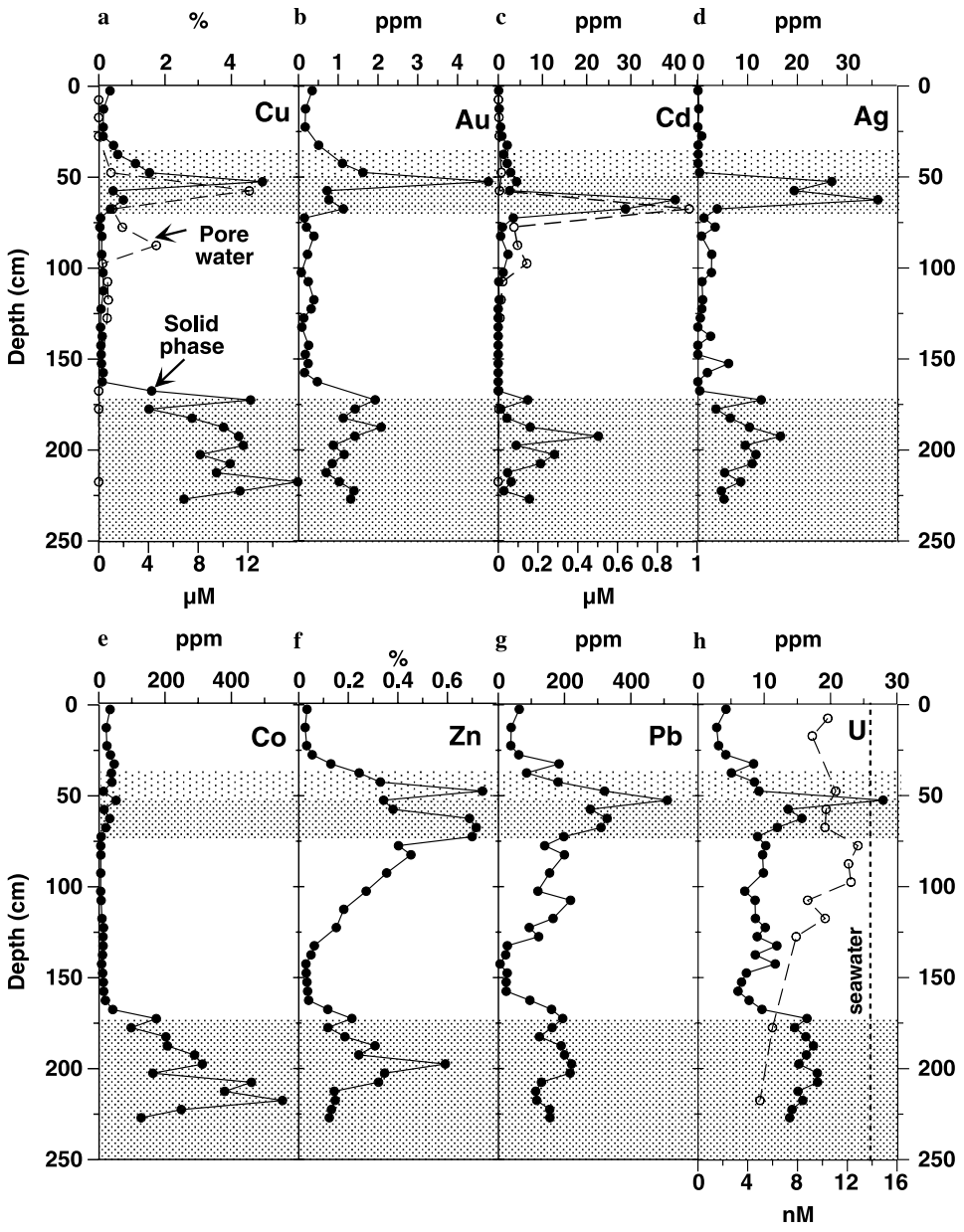

Fig. 6. Down core distribution of (a) solid and pore fluid Cu, (b) solid phase Au, (c) solid phase and pore fluid Cd, (d) solid phase Ag, (e) solid phase Co, (f) solid phase Zn, (g) solid phase Pb and, (h) solid and pore fluid U, dashed lines show seawater U value. Filled circles represent solid phase data, open circles represent pore fluid data from core CD102/43.

(70–165 cm) took place during or shortly after the last period of high-temperature activity of the Southern Mound, when low temperature fluids would have been pervasive in the vicinity of the vents (e.g., James and Elderfield, 1996; Schultz et al., 1996). Hence, elevated concentrations of pore water Mn^{2+} and Fe^{2+} below depths of 47.5 and 57.5 cm, respectively, are more consistent with release of these elements during in situ reduction and dissolution of oxidised minerals rather than any percolation of reduced hydrothermal fluids. The dissolved metal profiles (Figs. 3b and c) suggest that the core is suboxic/anoxic below a depth of 50 cm. The Fe and Mn zonation follows the thermodynamically predicted sequence for terminal electron acceptors, where Mn(IV) reduction precedes Fe(III) reduction as more energy is derived from the former reaction (Froelich et al., 1979). Solid phase Fe and Mn profiles indicate oxidation of upward diffusing dissolved Fe^{2+} and Mn^{2+} and precipitation in the oxic carbonate cap (Figs. 3b and c). This is supported by the observation in XRD scans of peaks in rhodochrosite ($MnCO_3$) and amorphous Fe-Mn-oxides at a depth of ~30 cm within the carbonate cap (0.74% Mn).

Surficial Mn-mineral enrichments occur widely across the TAG area (Scott et al., 1978; Metz et al., 1988; Mills et al., 2001), and Goulding et al. (1998) report Mn enrichments of up to 15% in the upper part of sediments from the southeastern flank of the active TAG mound. Fe/Mn-crusts are also present in the relict *Mir* and *Alvin* zones

(Mills et al., 2001) and significant (several %) enrichments were observed in near surface sediments of cores retrieved adjacent to the core studied here. Hence, there is significant heterogeneity in Mn transport and reaction across the TAG field, and core CD102/10 Mn diagenesis and reaction is probably diffusion controlled and therefore exhibits lower Mn concentrations (<1%) than other areas of the TAG field.

The solid phase Mn content of the transition zone and carbonate cap is similar to that in suboxic sediments from the equatorial Atlantic (Thomson et al., 1996; Mangini et al., 2001) but is significantly higher than that for the background core (<0.1% Mn throughout). However, while the highest pore water Mn^{2+} concentrations (3.8 μM) are significantly higher than the control site (maximum $Mn^{2+} = 0.078$ μM) they are much lower than values for sub-oxic pelagic sediments (~100 μM; Klinkhammer, 1980) or low-temperature fluids upwelling through TAG sediments (~150 μM; Mills et al., 1996). Hence, it is likely that Mn(II) production through reductive processes is limited by the low organic carbon content of the sediment.

The elevated pore water SO_4^{2-} values (Fig. 3a) could be attributed to oxidation of sulphides. Sulphide oxidation may occur aerobically within the oxic carbonate cap (see below), but anaerobic pathways must account for the excess SO_4^{2-} that occurs deeper in the sediment because of the presence of dissolved Fe^{2+} and Mn^{2+}. Anaerobic pyrite oxidation can occur inorganically in organic carbon rich sediments by concomitant reduction of MnO_2 (Aller and Rude, 1988; Schippers and Jørgensen, 2001, 2002), and Schippers and Jørgensen (2001) suggested that such a reaction pathway may also be of importance in hydrothermal sediments. The stoichiometry of this reaction produces 7.5 mol of Mn^{2+} for every mole of FeS_2 oxidised implying that significant Mn^{2+} levels should be present if this pathway is significant. The low pore water Mn^{2+} levels (2–4 μM) are not consistent with anaerobic MnO_2 oxidation of sulphides as a significant pathway to produce the SO_4^{2-} excess of ~4 mM observed in the lower part of the core. Further, Schippers and Jørgensen (2002) demonstrated that amorphous Fe(III)-oxides are unlikely to be important direct chemical oxidants for FeS_2 in marine sediments. Another mechanism for the elevated SO_4^{2-} values within anaerobic sediment might be dissolution of minor sulphate ($CaSO_4{\cdot}nH_2O$) phases present in sulphidic sediments at TAG (Little et al., 2004).

5.2. Sediment pH conditions

pH is a key variable in many diagenetic reactions and an accurate measure of this parameter is critical in a discussion of the relative importance of microbial and inorganic processes (see Section 5.3). Hannington et al. (1990a,b) measured pH values in pore waters from sulphidic and Fe-oxide cores from the active TAG mound of 3.5–5.5 and 6.8–7.3, respectively. Similarly, Bach and Edwards (2003) used a pH of 7.75 measured in pore waters from sediments from ODP hole 1024 in the vicinity of the ridge flank hydrothermal system (Elderfield et al., 1999) to constrain the energy yield from microbially mediated diagenetic reactions. However, these measurements were made on pore waters extracted from sediments (Hannington, personnel communication, 2004; Wheat and Mottl, 2000) and this technique frequently yields inaccurate pH data due to the temperature and pressure dependence of the dissociation constants of protonated species (Wheat and Mottl, 2000; Cruse and Seewald, 2001).

Thermodynamic calculations can be used to derive pH values in hydrothermal systems, either by assuming equilibrium with respect to solid phases, or from calculations of conservative mixing between seawater and end member hydrothermal fluids (e.g., McCollom and Shock, 1997). We can use the dissolved and solid phase geochemistry and mineralogy of the sediments to place limits on the pH (~5.5) at the elevated temperatures implied by the nontronite data (Fig. 7b). Alternatively, a temperature range of 60–85 °C (from the in situ temperature inferred from the nontronite data; Severmann et al., 2004) would imply a pH of ~5.8 in the intermediate layer if simple mixing of

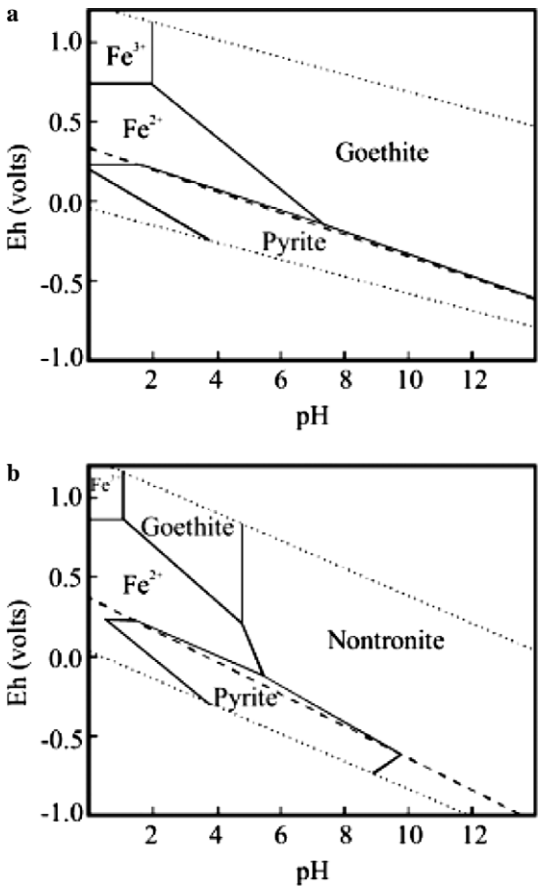

Fig. 7. Eh-pH diagrams illustrating Fe speciation for (a) 2 °C (pyrite and goethite as permitted solid phases) and (b) 85 °C (pyrite, goethite and nontronite as permitted stable phases). The activities of dissolved species are taken from the values measured in pore fluids in the intermediate layer. The Eh-pH diagrams were constructed using the data base of Johnson et al. (1992).

end member fluids with seawater is controlling ambient conditions (McCollom and Shock, 1997). Although the thus calculated pH may vary for different end member fluid compositions, the fluid chemistry of the EPR 21°N OBS vent site used by McCollom and Shock (1997) is very similar to the chemistry of the TAG end member fluids (Edmond et al., 1995).

We can also reconstruct the pH of low-temperature hydrothermal fluids from measurements of alkalinity and total CO_2 from gas tight samples (Sansone et al., 1998), which produce a pH of 5.5 for the 64 °C Baby Bare ridge flank hydrothermal fluids (using the carbonate equilibria described by Zeebe and Wolf-Gladrow (2001)).

While none of these approaches yields an unambiguous and unique solution to reconstructing the pH value of pore waters, we can place some constraints on pH values at different depths and different times within the sediment core studied here. The presence of carbonate is restricted to the upper portion of the core where it acts as a buffer to keep the pH at ~7.8. The pH of the fluids in the intermediate layer during nontronite formation was likely within the range ~5.5. The implications of this analysis are that fluids forming the intermediate Fe oxysilicate layer are similar in composition (pH ~ 5.5, anoxic, dissolved Fe^{2+} ~100 μM) to Baby Bare ridge flank fluids that may represent a high-temperature end-member of ridge flank hydrothermal fluids.

The pH of the fluids in the two sulphide layers is less well constrained. The absence of iron oxide and nontronite in these layers implies that the pH was less than ~7, and may have been as low as ~2 (Fig. 7a). The presence of low pH fluids in the upper sulphide layer is also supported by the presence of atacamite, which forms when cuprous chloride complexes and Cu^{2+} ions are released from sulphides during corrosion by acidic pore-fluids (Hannington, 1993).

5.3. The role of prokaryotes in sediment diagenesis

This sediment core contains a range of microbial niches from fully oxic carbonate sediment, through a sharp redox and pH gradient to suboxic/anoxic, low pH environments in metal-sulphide rich sediment. The total prokaryotic population is similar to that of the nearby carbonate control core CD102/10. Hence, it appears that the prokaryotes in the metalliferous sediment are not inhibited by—and are probably well adapted to— high metal content. In addition, the elevated populations in the upper sulphide layer, combined with distribution of redox sensitive metals in and around this zone, suggests that some prokaryotes are directly involved in metal metabolism. Although the prokaryotic numbers are lower compared to other deep sediments, the relatively high thymidine incorporation rates and high FDDC in core CD102/43 (Fig. 4) both suggest they are actively growing and well adapted to their environment.

The high pore water SO_4^{2-} levels, low organic carbon content and low concentration of AVS in the sediments all suggest absence of significant bacterial SO_4^{2-} reduction. However, sensitive radiotracer measurements demonstrate that limited sulphate reduction is occurring particularly in the transition zone (Fig. 5c). The maximum SRR in the transition zone broadly coincides with a maximum in pore water acetate concentrations and acetate utilisation (Figs. 5d and e). Acetate is a key intermediate in organic matter breakdown and is an important electron donor for SO_4^{2-}-reducing bacteria in marine sediments (Sørensen et al., 1981). However, the acetate utilisation rate at this depth (50 pmol/cm^3/d) is orders of magnitude lower than the SO_4^{2-} reduction rates (67 nmol/cm^3/d), hence there is likely to be an additional (unidentified) electron donor driving this reaction.

Sulphate reducers are generally considered to be obligate anaerobes, and hence it appears counterintuitive to observe the highest SRR in the oxic to suboxic transition zone (Fig. 5). However, Jørgensen and Bak (1991) have previously reported high SRR from oxic surface sediments. High SRR in near surface sediment may indicate anoxic conditions at least locally (micro environments) in the transition zone (Fig. 2). The potential role of micro environments and sediment heterogeneity is further supported by the large range in SRR measured in the triplicate syringe subcores from this depth section.

The elevated concentrations of pore water Fe^{2+} deeper in the core also indicate anaerobic conditions. SRR are much lower here, suggesting that Fe^{2+} is liberated by microbial Fe(III) reduction, which dominated over SO_4^{2-} reduction as the favoured terminal electron accepting process and is consistent with the presence of substantial numbers of Fe(III)-reducing microorganisms (Fig. 5a). Indeed, Fe reducing microorganisms may have a competitive advantage of SO_4^{2-} reducers in these sediments because of the high abundance of poorly crystalline metal oxides, and dissimilatory Fe reduction is favoured over SO_4^{2-} reduction (Lovley and Phillips, 1987).

Culturable Fe(III)-reducers were present even in the carbonate cap and maximum MPNs were measured at the same depth as maximum SRR, although there is little pore water Fe^{2+}. We suggest that microbial Fe(III)-reduction may be occurring in the top of the core and the Fe^{2+} produced is not accumulating, but is re-oxidised immediately. As some Fe(III)-reducing bacteria can also reduce SO_4^{2-} (Coleman et al., 1993) it is possible that these organisms are also responsible for the observed sulphate reduction.

Fe and Mn reducing prokaryotes are both present at depth within the core (Figs. 5a and b). In addition, except for the top ~50 cm for Fe(III)-reducers (see above), there is coincidence of distribution of metal reducing microorganisms with the corresponding reduced metal profiles, which suggests that metal reducing microorganisms are active in the sediment. However, despite the fact that Fe-oxides and authigenic Fe-oxysilicates comprise >50% of the bulk sediments in the intermediate layer, pore water Fe^{2+} levels are low (maximum 93.3 μM) relative

to those from suboxic continental margin sediments. In continental margin sediments the mechanism of Fe-mobilisation can be either bacterial Fe(III) reduction (Canfield et al., 1993a) or reductive dissolution by hydrogen sulphide (Thamdrup and Canfield, 1996). Pore water Fe concentrations can reach >200 μM in the presence of much lower solid phase Fe abundance (Sørensen and Jørgensen, 1987; Shaw et al., 1990; Canfield et al., 1993b; Thamdrup et al., 1994). The low pore water Fe^{2+} levels in the CD102/43 cannot be ascribed to large-scale contemporaneous uptake of Fe(II) into the authigenic phases present in the sediment as $\delta^{18}O$ studies (Severmann et al., 2004) indicate that nontronite (the major authigenic Fe-rich phase) formed at 60–85 °C, whereas the sediment was at the ambient temperature (2 °C) when recovered. Other authigenic Fe(II) mineral phases, such as FeS or $FeCO_3$, have low abundance or are absent. Hence, the low pore water Fe(II) concentrations are interpreted to arise from limited availability of electron donor for the bacterial reduction of Fe(III) and SO_4^{2-} in these metalliferous sediments. Interestingly, there is a strong correspondence between the depth profile of Fe(III)-reducing microorganisms and acetate utilization (Figs. 5a and e), suggesting that acetate is an important, albeit limited, substrate for Fe(III) as it is in other environments (Lovley and Chapelle, 1995).

In summary, although MPN results and microbial activity measurements demonstrate the presence of heterotrophic prokaryotes and processes, we believe that heterotrophy is only of limited importance in these organic-poor sediments. This is in contrast to the hydrothermal sediments of Guaymas Basin, where organic carbon contents of up to 4% (Simoneit et al., 1979) stimulate SRR in excess of 1500 nmol/cm^3/d (Elsgaard et al., 1994) and intense metal mobilisation (Cruse and Seewald, 2001).

5.4. Fe(II) oxidation—microbially mediated or abiotic?

Fe-oxide precipitation and nontronite formation in hydrothermal settings have been associated with bacterial intervention, either indirectly by microbial cell walls and exopolymers acting as a template for nucleation and layered silicate formation (Konhauser and Urrutia, 1999; Ueshima and Tazaki, 2001), or by direct involvement of Fe-oxidising bacteria (Alt, 1988; Köhler et al., 1994; Emerson and Moyer, 2002) such as *Acidothiobacillus*, *Acidomicrobium*, *Ferrimicrobium Leptospirillium*, *Sulfobacillus* and *Thiobacillus* (Madigan et al., 2003). Inorganic Fe(II) oxidation is rapid at ambient bottom water conditions (i.e., neutral pH, high O_2 concentrations), and any microbial oxidation of Fe(II) must therefore occur over comparable time scales in order to be utilised for growth. The kinetics of Fe(II) oxidation is strongly dependent on pH and O_2 and is highly nonlinear below pH 6 (Millero et al., 1987). The half life for oxidation of Fe(II) is 2–3 min in oxygenated Atlantic seawater, but increase to >1 year at pH <6 and oxygen levels <1 μM (Millero et al., 1987). Hence, the kinetic inhibition of inorganic Fe(II) oxidation at low pH offers the opportunity for microbial catalysis and utilisation of the energy released during oxidation of Fe(II) species.

Fe-oxidising microorganisms are ubiquitous in hydrothermal environments where there are sharp redox and oxygen gradients, together with a supply of Fe(II) in dissolved and particulate forms (Juniper and Tebo, 1995; Edwards et al., 2003a). Indeed, recent studies have shown that neutrophilic Fe-oxidising microorganisms make an important contribution to Fe oxidation at the Loihi seamount vent sites (Emerson and Moyer, 2002). However, because of the competition from abiotic Fe-oxidation, microbial Fe-oxidation at neutral pH requires microaerophilic conditions (Emerson and Moyer, 1997, 2002; Edwards et al., 2003b). Intensive microbial Fe-oxidation has also been reported from sulphide-rich ore-bodies that undergo weathering on land (Nordstrom and Southam, 1997). Oxidative dissolution of pyrite generates net acidity, so the microorganisms that are capable of catalysing the oxidation of Fe or S in these deposits need to be adapted to very low pH (Norris, 1990; Hallmann et al., 1992; Leduc and Ferroni, 1994; Schrenk et al., 1998; Edwards et al., 1999). Based on thermodynamic considerations, microorganisms that use ferrous Fe as the sole energy source predominantly use oxygen as electron acceptor (Johnson, 1998). Consequently, Fe oxidation in acidic environments requires high ambient oxygen concentrations, whereas we infer low oxygen concentrations in the buried sulphide deposits from TAG.

As significant cell concentrations are present in the pelagic cap of core CD102/43 (0–35 cm) they were also likely to have been present during deposition of the Fe-oxysilicate layer (50–165 cm) when carbonates were replaced by Fe-oxysilicates during interaction with Fe-rich low-temperature hydrothermal fluids. Positive enrichments from a neighbouring core from the TAG site demonstrated the presence of presumptive Fe-oxidising prokaryotes in hydrothermal sediments from this area (metal oxidising MPN's were not conducted for CD102/43). However, the presence of such microorganisms does not prove they play a major role in Fe(II) oxidation. The ability of chemolithotrophic microorganisms to compete with abiotic oxidation is not solely a function of reaction kinetics, but also of the free energy yield of the reaction which is required for growth and/or cellular maintenance (Roden et al., 2002; Sobolev and Roden, 2004).

To illustrate the effect of a key variable, pH, on prokaryotic Fe(II) oxidation in this environment the free energy yield for the formation of various metal oxide phases from dissolved Fe^{2+} was calculated over the pH range 2–8 (encompassing the entire pH range discussed in Section 5.2) and temperature range of 2–100 °C (Fig. 8). Calculations were based on the following reactions:

$$\text{Magnetite } 3Fe^{2+} + 0.5O_2 + 3H_2O \Longleftrightarrow Fe_3O_4 + 6H^+ \quad (1)$$

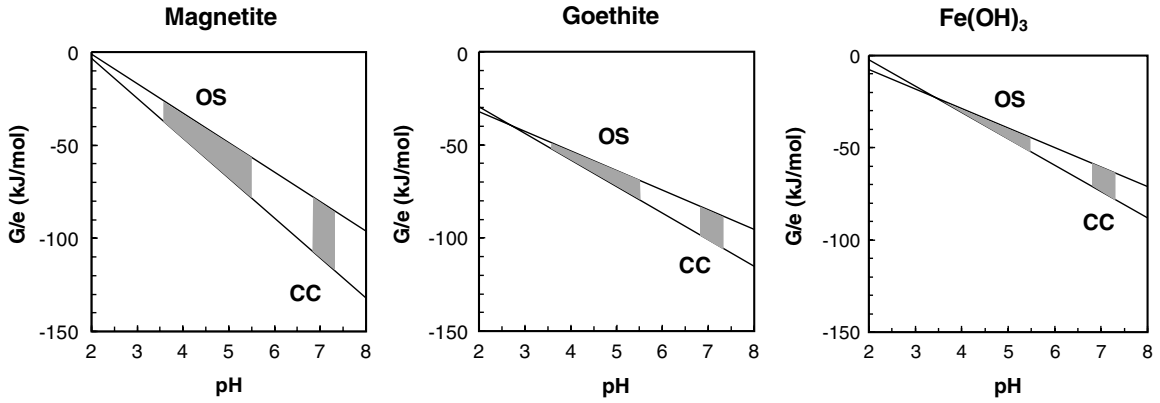

Fig. 8. Calculated free energy yield for the formation of magnetite, goethite and $Fe(OH)_3$ from dissolved Fe^{2+} as a function of pH. The upper and lower lines for each mineral phase were calculated at temperatures of 2 °C (the in situ temperature at the time the core was collected) and 100 °C (the upper limit for formation on nontronite in the intermediate layer (Severmann et al., 2004)), respectively. The grey box labelled OS refers to the pH range observed in sediments containing oxidised sulphides, whereas the grey box labelled CC refers to the pH in the overlying carbonate cap (Hannington et al., 1990a,b).

$$\text{Goethite } Fe^{2+} + 0.25O_2 + 1.5H_2O \Longleftrightarrow FeOOH + 2H^+ \quad (2)$$

$$Fe(OH)_3\ Fe^{2+} + 0.25O_2 + 2.5H_2O \Longleftrightarrow Fe(OH)_3 + 2H^+ \quad (3)$$

These calculations were carried out using the average in situ pore water Fe^{2+} concentration of 30 μM in core CD102/43 (i.e., assuming all dissolved Fe present as Fe^{2+}) and a dissolved O_2 concentration of 1 μM. Although we do not have measurements of dissolved O_2 levels, a value of 1 μM was chosen to allow comparison with the study of Bach and Edwards (2003), who also used this value in their calculations (see below). A factor of three variation in dissolved Fe^{2+} levels would result in a difference of 3–5 kJ/mol in the calculated ΔG/e (ΔG normalised per electron transferred) values at any particular pH value, whereas a variation of two orders of magnitude in the dissolved O_2 concentrations are required to achieve a similar variation in ΔG/e. At a pH range for sulphidic sediments of 3.8–5.5 and a temperature of 2 °C, ΔG/e for the formation of $Fe(OH)_3$ ranges from only −22.7 to −40.6 kJ/mol. The energy required to synthesise 1 mol of ATP under conditions presumed to prevail in an actively growing cell is 50–70 kJ, and many anaerobic microorganisms require energy that is equivalent to one-third of an ATP unit (i.e., −20 kJ/mol) to exploit the free energy released in a reaction (Schink, 1997). These low energy yields, coupled with the low Fe^{2+} concentrations in the pore waters (50–90 μM) suggest that the balance between abiotic and microbiological control over oxidation of Fe^{2+} is finely poised below the sharp redox gradient in the upper sulphide layer. However, the significant increase in total prokaryotic populations in the upper sulphide layer demonstrates that microorganisms obtain significant energy from catalysing reactions in this layer (Fig. 4), but not in the deeper sulphide layer which is remote from influence of oxic, near neutral pH seawater and where there is no equivalent increase in total microbial numbers. It may be that Fe(II) oxidisers are able to utilise energy yields below −20 kJ/mol, like some other bacteria (Jackson and McInerney, 2002) or that pore water pH is higher than 3.8–5.5, but low prokaryotic cell numbers and thymidine incorporation both point to limited prokaryotic production, and hence suggest a dominance of abiotic over biotic Fe-oxidation.

5.5. The role of prokaryotes in trace metal diagenesis

Cu, Au and Cd show sharp solid phase and pore water peaks in the upper sulphide layer. Cu is associated with chalcopyrite in both sulphide layers and with atacamite in the upper sulphide layer and the transition zone. Atacamite is commonly associated with alteration of chalcopyrite at the sediment–water interface, and studies of the active TAG mound have shown that atacamite contains grains of native gold (Hannington et al., 1991; Herzig et al., 1991; Tivey et al., 1995). We also identified an association between native gold and atacamite in core CD102/43. Hence, it is likely that the supergene enrichment of Cu and Au in the upper sulphide layer is associated with the active prokaryotic diagenesis occurring in this layer. The coincidence of the pore water and solid phase peaks of Cu and Cd indicates that there is ongoing remineralisation of Cu and Cd bearing phases in the upper sulphide layer. The sequence of metal dissolution with increasing depth in the upper sulphide layer is Mn → Cu/Au → Cd → Fe. This sequence follows the model of standard energy potential in suboxic sediments, and accords with previous observations for metal enrichments in organic-rich deep-sea sediments (Thomson et al., 1998). This zonation suggests there is a gradient in redox conditions in the upper sulphide layer that drives the diagenesis of metals and alteration of sulphide minerals in association with prokaryotic processes. The lack of an equivalent process in the lower sulphide layer is because this lower zone is not in contact with the oxic

carbonate sediments, and thus there is no systematic redox gradient.

The Zn data show evidence of diagenetic remobilisation in the upper sulphide layer and surrounding sediment (Fig. 6f). This is likely a result of the low pH conditions generated by sulphide oxidation, as indicated by an increase in sulphate concentrations above the upper sulphide zone (Fig. 3). Precipitation of fine-grained secondary sphalerite has been linked to the activity of sulphate reducing bacteria (Labrenz et al., 2000; Edwards et al., 2003b), and fits with the observation that elevated SRR occur in the transition zone immediately above the upper sulphide layer (Fig. 5c). Hence, it is likely that Zn remobilised from the upper sulphide layer diffuses into the overlying transition zone where reaction with sulphide produced by bacterial sulphate reduction results in the precipitation of secondary sphalerite. The Pb solid phase distribution closely follows that of Zn (Fig. 6g), suggesting close coupling between these elements during S-cycling (dissolution, transport and reaction with sulphide). Ag is enriched in both sulphide layers, with concentrations of up to 36 ppm in the upper sulphide layer. Ag transport has been linked to that of Zn in the active TAG mound (Tivey et al., 1995), but although the highest concentrations of both Zn and Ag are observed in the upper sulphide layer, there is no apparent redistribution of Ag into adjacent sediment layers.

Solid phase U levels are high throughout the core, with elevated U contents in both sulphide layers (>10 ppm). High U levels (up to 20 ppm) have also been observed in the active TAG mound (Mills et al., 1994). U enrichments are localised within submicron sized particles on pyrite grains (Figs. 9a and b). The largest U enrichment is in a discrete zone at the top of the upper sulphide layer, coincident with the maximum gradient in dissolved Mn^{2+} and active redox processes. U is likely present in an amorphous phase, rather than as a discrete U-mineral, and the sub-micron size and surface association of U is consistent with prokaryotic mediation of the U enrichment (Mills et al., 1994). Indeed, prokaryotic U(VI) reduction is associated with Fe(III) reduction in experiments with natural populations of microbes (Lovley et al., 1991, 1993; Kashefi and Lovley, 2000; Holmes et al., 2002), and here the maximum peak in U enrichment is close to a maximum in Fe(III)-reducing prokaryotes (125 cell/cm^3, Figs. 5 and 6). The U pore water data show evidence of U uptake throughout the core (Fig. 6h), and Fe(III)-reducing prokaryotes are also present throughout. The greatest depletion of pore water U (relative to seawater values) is observed in the lower sulphide layer (~5 nM), coincident with the highest Fe(II) levels in the pore waters and the second highest population of Fe(III)-reducing prokaryotes (99 cell/cm^3). Hence, we suggest that U fixation via reduction occurs concomitantly with microbial Fe reduction (Fig. 5a) and is associated with pyrite surfaces (Fig. 9), where the most effective Fe-cycling occurs in these sediments.

6. Conclusions

We conclude that there is a specialised microbial community in these hydrothermal sediments, which appears to be resistant to the high concentrations of toxic metals. Despite the presence of large pools of suitable reduced inorganic electron donors, there is little evidence for significant overall enhancement of microbial activity in this environment. However, microbial processes and populations are stimulated in the buried sulphide layer (50–70 cm) and the transition zone above. This is related to Zn, Pb, Cu, Au, Ag, Cd, U remobilization and precipitation. Populations of Fe(III)- and Mn(IV)-reducing prokaryotes increase at depth and correspond with increases in pore water Fe^{2+} and Mn^{2+} and continuing removal of dissolved U.

In view of the high concentration of reduced minerals in hydrothermal sediments and in the ocean crust, in general, their potential as important microbial habitats has been subject to several studies. These have suggested that microorganisms play a major role in the weathering of seafloor massive sulphide deposits (Wirsen et al., 1993, 1998; Eberhard et al., 1995; Edwards et al., 2003a) and that microbial oxidation can support high levels of biomass production in the ocean crust (Bach and Edwards, 2003). However, our observations and thermodynamic calculations suggest that the free energy available from Fe-oxidation may limit

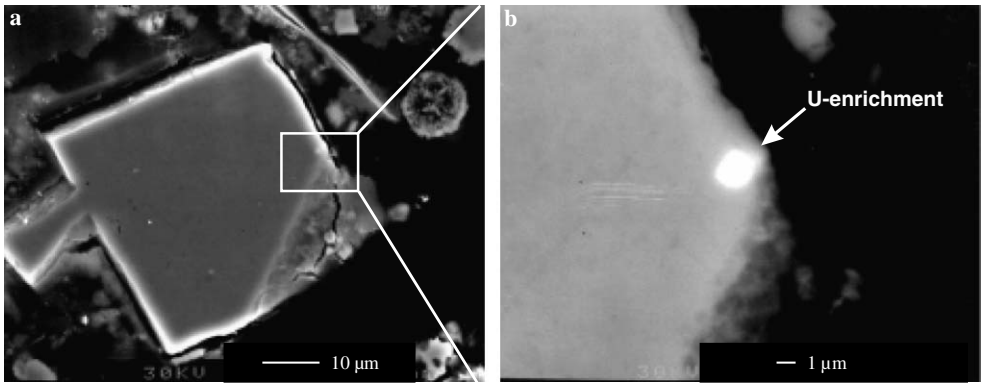

Fig. 9. (a) and (b) BSEI SEM images of U enrichment on the surface of a pyrite grain within the upper sulphide layer. Brightness is directly related to average atomic mass and is sensitive to large U enrichments which were confirmed by EDAX analysis.

microbial activity at the low pH and low effective electron acceptor (O_2) concentrations present deep in the subsurface of the hydrothermal sediments and in the deep ocean crust (Hannington et al., 1990a,b; Sansone et al., 1998). Hence, we believe that it is likely that the dominant role of prokaryotes may be in surface and shallow subsurface weathering of seafloor massive sulphide deposits and ocean crust, in the absence of significant subsurface fluid flow.

Acknowledgments

We are grateful to captain and crew of RVS Charles Darwin for their assistance during the BRIDGE Cruise CD 102. Particular thanks for M. Rudnicki and J. Rhodes for help with shipboard and other analyses. This research was funded by the Natural Environmental Research Council, UK, BRIDGE Programme and the Leverhulme Trust.

Associate editor: Jan P. Amend

References

Aller, R.C., Rude, P.D., 1988. Complete oxidation of solid phase sulfides by manganese and bacteria in anoxic marine sediments. *Geochim. Cosmochim. Acta* **52**, 751–765.

Alt, J.C., 1988. Hydrothermal oxide and nontronite deposits on seamounts in the Eastern Pacific. *Mar. Geol.* **81**, 227–239.

Bach, W., Edwards, K.J., 2003. Iron and sulfide oxidation within the basaltic ocean crust: Implications for chemolithoautothrophic microbial biomass production. *Geochim. Cosmochim. Acta* **67**, 3871–3887.

Bethke, C.M., 1996. *Geochemical Modelling*. Oxford University Press, Oxford, UK.

Bottrell, S.H., Parkes, R.J., Cragg, B.A., Raiswell, R., 2000. Isotopic evidence for anoxic pyrite oxidation and stimulation of bacterial sulfate reduction in marine sediments. *J. Geol. Soc. London* **157**, 711–714.

Canfield, D.E., Jørgensen, B.B., Fossing, H., Glud, R., Gundersen, J., Ramsing, N.B., Thamdrup, B., Hansen, J.W., Nielsen, L.P., Hall, P.O.J., 1993a. Pathways of organic-carbon oxidation in 3 continental-margin sediments. *Mar. Geol.* **113**, 27–40.

Canfield, D.E., Thamdrup, B., Hansen, J.W., 1993b. The anaerobic degradation of organic matter in Danish coastal sediments: Iron reduction, manganese reduction, and sulfate reduction. *Geochim. Cosmochim. Acta* **57**, 3867–3883.

Chen, J.H., Wasserburg, G.J., Damm, K.L.V., Edmond, J.M., 1986. The U-Th-Pb systematics in hot springs on the East Pacific Rise at 21° N and the Guaymas Basin. *Geochim. Cosmochim. Acta* **50**, 2467–2479.

Cline, J.D., 1969. Spectrophotometric determination of hydrogen sulfide in natural waters. *Limnol. Oceanogr.* **14**, 454–458.

Coleman, M.L., Hedrick, D.B., Lovley, D.R., White, D.C., Pye, K., 1993. Reduction of Fe(III) in sediments by sulphate-reducing bacteria. *Nature* **361**, 436–438.

Cragg B.A., Harvey S.M., Fry J.C., Herbert R.A., Parkes R.J., 1992. Bacterial biomass and activity in the deep sediment layers of the Japanese Sea, Hole 798B. In: Pisciotte, K.A., Ingle Jr. J.C., Breymann, M.T.v., Barron, J. (Eds.), Proc. ODP, Sci. Results, Vol. 127/128, Pt. 1, College station, pp. 761–776.

Cragg B.A. Parkes R.J., 1993. Bacterial profiles in hydrothermally active deep sediment layers from the Middle Valley (N.E. Pacific) Sites 857 and 858. In: Mottl, M.J., Davis, E.E., Fisher, A.T. (Eds.), Proc. ODP, Sci. Results, Vol. 139, College Station, pp. 509–516.

Cruse, A.M., Seewald, J., 2001. Metal mobility in sediment-covered ridge-crest hydrothermal systems: experimental and theoretical constraints. *Geochim. Cosmochim. Acta* **65**, 3233–3247.

Deming, J.W., Baross, J.A., 1993. Deep-sea smokers: windows to a subsurface biosphere? *Geochim. Cosmochim. Acta* **57**, 3219–3230.

D'Hondt, S., Jorgensen, B.B., Miller, D.J., Batzke, A., Blake, R., Cragg, B.A., Cypionka, H., Dickens, G.R., Ferdelman, T., Hinrichs, K.-U., Holm, N.G., Mitterer, R., Spivack, A., Wang, G., Bekins, B., Engelen, B., Ford, K., Gettemy, G., Rutherford, S.D., Sass, H., Skilbeck, C.G., Aiello, I.W., Guerin, G., House, C.H., Inagaki, F., Meister, P., Naehr, T., Niitsuma, S., Parkes, R.J., Schippers, A., Smith, D.C., Teske, A., Wiegel, J., Padilla, C.N., Acosta, J.L.S., 2004. Distributions of microbial activities in deep subseafloor sediments. *Science* **306**, 2216–2221.

D'Hondt, S., Rutherford, S., Spivak, A.J., 2002. Metabolic activity of subsurface life in deep-sea sediments. *Science* **295**, 2067–2070.

Eberhard, C., Wirsen, C.O., Jannasch, H.W., 1995. Oxidation of polymetal sulfides by chemolithoautotrophic bacteria from deep-sea hydrothermal vents. *Geomicrobiol. J.* **13**, 145–164.

Edmond, J.M., Campbell, G.A., Palmer, M.R., Klinkhammer, G.P., German, C.R., Edmonds, H.N., Elderfield, H., Thompson, G., Rona, P.A., 1995. Time series study of vent fluids from the TAG and MARK sites (1986, 1990) Mid-Atlantic Ridge: a new solution chemistry model and a mechanism for Cu/Zn zonation in massive sulphide orebodies. In: Parson, L.M., Walker, C.L., Dixon, D.R. (Eds.), *Hydrothermal Vents and Processes*. Geological Society Special Publication 87, pp. 77–86.

Edwards, K.J., Goebel, B.M., Rodgers, T.M., Schrenk, M.O., Gihring, T.M., Cardona, M.M., Hu, B., McGuire, M.M., Hamers, R.J., Pace, N., Banfield, J.F., 1999. Geomicrobiology of pyrite (FeS_2) dissolution: case study at Iron Mountain, California. *Geomicrobiol. J.* **16**, 155–179.

Edwards, K.J., McCollom, T.M., Konishi, H., Buseck, P.R., 2003a. Seafloor bioalteration of sulfide minerals: Results from in situ incubation studies. *Geochim. Cosmochim. Acta* **67**, 2843–2856.

Edwards, K.J., Rogers, D.R., Wirsen, C.O., McCollom, T.M., 2003b. Isolation and characterization of novel phsychrophili, neutrophilic, Fe-oxidizing, chemolithoautotrophic α- and γ-proteobacteria from the deep sea. *Appl. Environ. Microbiol.* **69**, 2906–2913.

Elderfield, H., Wheat, C.G., Mottl, M.J., Monnin, C., Spiro, B., 1999. Fluid and geochemical transport through oceanic crust: a transect across the eastern flank of the Juan de Fuca Ridge. *Earth Planet. Sci. Lett.* **172**, 151–165.

Elsgaard, L., Isaksen, M.F., Jørgensen, B.B., Alayse, A.-M., Jannasch, H.W., 1994. Microbial sulfate reduction at the Guaymas Basin hydrothermal vent area: influence of temperature and substrate. *Geochim. Cosmochim. Acta* **58**, 3335–3343.

Emerson, D., Moyer, C.L., 1997. Isolation and characterisation of novel iron-oxidizing bacteria that grow at circumneutral pH. *Appl. Environ. Microbiol.* **60**, 4032–4038.

Emerson, D., Moyer, C.L., 2002. Neutrophilic Fe-oxidizing bacteria are abundant at the Loihi Seamount hydrothermal vents and play a major role in Fe oxide deposition. *Appl. Environ. Microbiol.* **68**, 3085–3093.

Emerson, S., 1985. Organic carbon preservation in marine sediments. In: Sundquist, E.T., Broecker, W.S. (Eds.), *The Carbon Cycle and Atmospheric CO2: Natural Variations Archean to Present*, Vol. 32, American Geophysical Union.

Fallick, A.E., Aston, J.H., Boyce, A.J., Ellam, R.M., Russell, M.J., 2001. Bacteria were responsible for the magnitude of the world class hydrothermal base metal sulfide orebody at Navan. *Econ. Geol.* **96**, 885–890.

Fortin, D., Ferris, F.G., Beveridge, T.J., 1997. Surface-mediated mineral development by bacteria. In: Banfield, J.F., Nealson, K.H. (Eds.), *Geomicrobiology: Interactions Between Microbes and Minerals*, Vol. 35. Mineralogical Society of America, pp. 161–177.

Froelich, P.N., Klinkhammer, G.P., Bender, M.L., Luedtke, N.A., Health, G.R., Cullen, D., Dauphin, P., Hammond, D.E., Hartman, B., Maynard, V., 1979. Early organic matter in pelagic sediments of the eastern equatorial Atlantic: suboxic diagenesis. *Geochim. Cosmochim. Acta* **43**, 1075–1090.

German, C.R., Higgs, N.C., Thomson, J., Mills, R.A., Elderfield, H., Blusztajn, J., Fleer, A.P., Bacon, M.P., 1993. A geochemical study of

metalliferous sediment from TAG hydrothermal mound, 26°08′N, Mid-Atlantic Ridge. *J. Geophys. Res.* **98**, 9683–9692.

Getliff, J.M., Fry, J.C., Cragg, B.A., Parkes, R.J., 1992. The potential for bacterial growth in deep sediments layers of the Japan Sea, Hole 789B-Leg 128. In: Pisciotto, K.A., Ingle, J.C., von Breymann, M.T., Barron, J. et al. (Eds.), Proc. ODP, Sci. Results, Vol. 127/128. College station, pp. 755–759.

Goulding, H.C., Mills, R.A., Nesbitt, R.W., 1998. Precipitation of hydrothermal sediments on the active TAG mound: implications for ochre formation. In: Mills, R.A. Harrison, K. (Eds.), *Modern Ocean Floor Processes and the Geological Record*. Geological Society Special Publication 148, pp. 201–216.

Hallmann, R., Friedrich, A., Koops, H.-P., Pommering-Roser, A., Rhode, K., Zenneck, C., Sand, W., 1992. Physiological characteristics of Thiobacillus ferrooxidans and Leptospirillum ferrooxidans and physiochemical factors influence microbial metal leaching. *Geomicrobiol. J.* **10**, 193–206.

Hannington, M.D., 1993. The formation of atacamite during weathering of sulphides on the modern sea-floor. *Can. Min.* **31**, 945–956.

Hannington, M.D., Hall, G.E.M., Vaive, J., 1990a. Acid pore fluids from an oxidizing sulfide deposit on the Mid-Atlantic Ridge- Implications for supergene enrichment of gold on the seafloor. *Geol. Soc. America Annual Meeting* Program with Abstr., **22**(3), p. 42.

Hannington, M.D., Herzig, P.M., Thompson, G., Rona, P.A., 1990b. Metalliferous sulfide-oxide sediments from the TAG hydrothermal field (26oN), Mid-Atlantic Ridge. *EOS Trans. AGU 71 Fall Meet. Suppl.*, 1653.

Hannington, M.D., Herzig, P.M., Scott, S.D., Thompson, G., Rona, P.A., 1991. Comparative mineralogy and geochemistry of gold-bearing sulfide deposits on the mid-ocean ridges. *Mar. Geol.* **101**, 217–248.

Heath, G.R., Moore, T.C., Dauphin, J.P., 1977. Organic carbon in deep-sea sediments. In: Anderson, N.R., Malahoff, A. (Eds.), *The fate of fossil fuel CO_2 in the oceans*. Plenum Press, New York, pp. 605–625.

Herzig, P.M., Hannington, M.D., Scott, S.D., Maliotis, G., Rona, P.A., Thompson, G., 1991. Gold-rich seafloor gossans in the Troodos ophiolite and on the Mid-Atlantic Ridge. *Econ. Geol.* **86**, 1747–1755.

Holden, J.F., Summit, M., Baross, J.A., 1998. Thermophylic and hyperthermophilic mircoorganism in 3–30 °C hydrothermal fluids following a deep-sea volcanic eruption. *FEMS Micobiol. Ecol.* **25**, 33–41.

Holmes, D.E., Finneran, K.T., O'Neil, R.A., Lovley, D.R., 2002. Enrichment of members of the family Geobacteraceae associated with stimulation of dissimilatory metal reduction in uranium-contaminated aquifer sediments. *Appl. Environ. Microbiol.* **68**, 2300–2306.

Humphris, S.E., Herzig, P.M., Miller, D.J., Alt, J.C., Becker, K., Brown, D., Brugmann, G., Chiba, H., Fouquet, Y., Gemmell, J.B., Guerin, G., Hannington, M.D., Holm, N.G., Honnorez, J., Iturrino, G.J., Knott, R., Ludwig, R., Nakamura, K., Petersen, S., Reysenbach, A.-L., Rona, P.A., Smith, S., Sturz, A.A., Tivey, M.K., Zhao, X., 1995. The internal structure of an active sea-floor massive sulphide deposit. *Nature* **377**, 713–716.

Jackson, B.E., McInerney, M.J., 2002. Anaerobic microbial metabolism can proceed close ot thermodynamic limits. *Nature* **415**, 454–456.

James, R.H., Elderfield, H., 1996. The chemistry of ore-forming fluids and mineral formation rates in an active hydrothermal sulfide deposit on the Mid-Atlantic Ridge. *Geology* **24**, 1147–1150.

Jannasch, H.W., Mottl, M.J., 1985. Geomicrobiology of deep-sea hydrothermal vents. *Science* **229**, 717–725.

Johnson, D.B., 1998. Biodiversity and ecology of acidophilic microorganism. *FEMS Micobiol. Ecol.* **27**, 307–317.

Johnson, J.W., Oelkers, E.H., Helgeson, H.C., 1992. SUPCRT92: a software package for calculating the standard molal thermodynamic properties of minerals, gases, aqueous species, and reactions from 1 to 5000 bar and 0 to 1000 °C. *Comput. Geosci.* **18**, 899–947.

Jørgensen, B.B., 1983. Processes at the sediment-water interface. In: Bolin, E.B., Cook, R.B. (Eds.), *The Major Biogeochemical Cycles and Their Interactions*. John Wiley, pp. 477–515.

Jørgensen, B.B., Bak, F., 1991. Pathways and microbiology of thiosulphate transformations and sulfate reduction in a marine sediment (Kattegat,Denmark). *Appl. Environ. Microbiol.* **57**, 847–856.

Juniper, S.K., Tebo, B.M., 1995. Microbe-metal interactions and mineral deposition at hydrothermal vents. In: Karl, D.M. (Ed.), *The Microbiology of Deep-Sea Hydrothermal Vents*. CRC Press, Boca Raton, FL, pp. 219–253.

Kasama, T., Murakami, T., 2001. The effect of microorganism on Fe precipitation rates at neutral pH. *Chem. Geol.* **180**, 117–128.

Kashefi, K., Lovley, D.R., 2000. Reduction of Fe(III), Mn(IV), and toxic metals at 100 °C by *Pyrobaculum islandicum*. *Appl. Environ. Microbiol.* **66**, 1050–1056.

King, G.M., 1991. Measurements of acetate concentrations in marine pore waters by using an enzymatic approach. *Appl. Environ. Microbiol.* **57**, 3476–3481.

Klinkhammer, G.P., 1980. Early diagenesis in sediments from the eastern equatorial Pacific. II. Pore water metal results. *Earth Planet. Sci. Lett.* **49**, 81–101.

Köhler, B., Singer, A., Stoffers, P., 1994. Biogenic nontronite from marine white smoker chimneys. *Clays Clay Miner.* **42**, 689–701.

Konhauser, K.O., 1998. Diversity of bacterial iron mineralization. *Earth Sci. Rev.* **43**, 91–121.

Konhauser, K.O., Urrutia, M.M., 1999. Bacterial clay authigenesis: a common biogeochemical process. *Chem. Geol.* **161**, 399–413.

Koroleff, F., 1983. Determination of silicon. In: Grasshoff, K., Ehrhardt, M., Kremling, K. (Eds.), *Methods of Seawater Analysis*. Verlag Chemie, pp. 174–183.

Küsel, K., Roth, U., Drake, H.L., 2002. Microbial reduction of Fe(III) in the presence of oxygen under low pH conditions. *Env. Microbiol.* **4**, 414–421.

Labrenz, M., Druschel, G.K., Thomsen-Ebert, T., Gilbert, B., Welch, S.A., Kemner, K.M., Logan, G.A., Summons, R.E., De Stasio, G., Bond, P.L., Lai, B., Kelly, S.D., Banfield, J.F., 2000. Formation of sphalerite (ZnS) deposits in natural biofilms of sulfate-reducing bacteria. *Science* **290**, 1744–1747.

Lalou, C., Reyss, J.L., Brichet, E., Rona, P.A., Thompson, G., 1995. Hydrothermal activity on a 10^5-year scale at a slow-spreading ridge, TAG hydrothermal field, Mid-Atlantic Ridge 26°N. *J. Geophys. Res.* **100**, 17,855–17,862.

Leduc, L.G., Ferroni, G.D., 1994. The chemolithotrophic bacterium *Thiobacillus ferroxidans*. *FEMS Microbiol. Rev.* **14**, 103–120.

Little, C.T.S., Glynn, S.E.J., Mills, R.A., 2004. Four hundred and ninety million year record of bacteriogenic iron oxide precipitation at deep-sea hydrothermal vents. *Geomicrobiol. J.* **21**, 415–429.

Lovley, D.R., Chapelle, F.H., 1995. Deep subsurface microbial processes. *Rev. Geophys.* **33**, 365–381.

Lovley, D.R., Phillips, E.J.P., 1987. Competitive mechanism for inhibition of sulfate reduction and methane production in the zone of ferric iron reduction in sediments. *Appl. Environ. Microbiol.* **53**, 2636–2641.

Lovley, D.R., Phillips, E.J.P., Gorby, Y.A., Landa, E.R., 1991. Microbial reduction of uranium. *Nature* **350**, 413–416.

Lovley, D.R., Roden, E.E., Phillips, E.J.P., Woodward, J.C., 1993. Enzymatic iron and uranium reduction by sulfate-reducing bacteria. *Mar. Geol.* **113**, 41–53.

Madigan, M.T., Martinko, J.M., Parker, J., 2003. *Brock Biology of Microorganisms*. Prentice-Hall Inc., Englewood Cliffs, NJ.

Malahoff, A., McMurtry, G.M., Wiltshire, J.C., Yeh, H.-W., 1982. Geology and chemistry of hydrothermal deposits from active submarine volcano Loihi, Hawaii. *Nature* **298**, 234–239.

Mangini, A., Jung, M., Laukenmann, S., 2001. What can we learn from peaks of uranium and manganese in deep sea sediments? *Mar. Geol.* **177**, 63–78.

McCollom, T.M., Shock, E.L., 1997. Geochemical constraints on chemolithoautotrophic metabolism by microorganisms in seafloor hydrothermal systems. *Geochim. Cosmochim. Acta* **61**, 4375–4391.

McMurtry, G.M., Wang, C.-H., Yeh, H.-W., 1983. Chemical and isotopic investigations into the origin of clay minerals from the Galapagos hydrothermal mound field. *Geochim. Cosmochim. Acta* **47**, 475–489.

Metz, S., Trefry, J.H., Nelsen, T.A., 1988. History and geochemistry of a metalliferous sediment core from the Mid-Atlantic Ridge at 26°N. *Geochim. Cosmochim. Acta* **52**, 2369–2378.

Millero, F.J., Sotolongo, S., Izaguirre, M., 1987. The oxidation kinetics of Fe(II) in seawater. *Geochim. Cosmochim. Acta* **51**, 793–801.

Mills, R.A., Alt, J.C., Clayton, T., 1996. Low-temperature fluid flow through sulfidic sediments from TAG: modification of fluid chemistry and alteration of mineral deposits. *J. Geophys. Res.* **98**, 3495–3498.

Mills, R.A., Elderfield, H., Thomson, J., 1993. A dual origin for the hydrothermal component in a metalliferous sediment core from the Mid-Atlantic Ridge. *J. Geophys. Res.* **98**, 9671–9681.

Mills, R.A., Thomson, J., Elderfield, H., Hinton, R.W., Hyslop, E., 1994. Uranium enrichment in metalliferous sediments from the Mid-Atlantic Ridge. *Earth Planet. Sci. Lett.* **124**, 35–47.

Mills, R.A., Wells, D.M., Roberts, S., 2001. Genesis of ferromanganese crusts from the TAG hydrothermal field. *Chem. Geol.* **176**, 283–293.

Nercessian, O., Fouquet, Y., Pierre, C., Prieur, D., Jeanthon, C., 2005. Diversity of Bacteria and Archaea associated with a carbonate-rich metalliferous sediment sample from the Rainbow vent field on the Mid-Atlantic Ridge. *Environ. Microbiol.* **7**, 698–714.

Nieuwnenhuize, J., Maas, Y.E.M., Middelburg, J.J., 1994. Rapid analysis of organic carbon and nitrogen in particulate materials. *Mar. Chem.* **45**, 217–224.

Nordstrom, D.K., Southam, G., 1997. Geomicrobiology of sulfide mineral formation. *Rev. Miner.* **35**, 361–390.

Norris, P.R., 1990. Acidophilic bacteria and their activity in mineral sulfide oxidation. In: Ehrlich, H.L., Brierley, C.L. (Eds.), *Microbial Mineral Recovery*. McGraw-Hill, New York, pp. 3–27.

Parkes, R.J., Buckingham, W.J., 1986. The flow of organic carbon through aerobic respiration and sulphate reduction in inshore marine sediments. In: *Proceedings of the 4th International Symposium on Microbial Ecology*, pp. 617–624.

Parkes, R.J., Cragg, B.A., Wellsbury, P., 2000. Recent studies on bacterial populations and processes in subseafloor sediments: a review. *Hydrogeol. J.* **8**, 11–28.

Rivera-Duarte, I., Flegal, A.R., 1996. Microtechniques for the determination of nanomolar concentrations of trace elements in $\leqslant$10 ml of sediment porewater. *Anal. Chim. Acta* **328**, 13–17.

Roden, E.E., Sobolev, D., Glazer, B., Luther, G.W., 2002. New insights into the biogeochemical cycling of iron in circumneutral sedimentary environments: potential for a rapid microscale bacterial Fe redox cycle at the aerobic-anaerobic interface. In: Coates, J.D., Zhang, C. (Eds.), *Iron in the Natural Environment: Biogeochemistry, Microbial Diversity, and Bioremedidation*. Kluwer Academic Publisher, Dordrecht (Hingham, MA).

Rona, P.A., Bogdanov, Y.A., Gurvich, E.G., Rimski-Korsakov, N.A., Sagalevitch, A.M., Hannington, M.D., Thompson, G., 1993. Relict hydrothermal zones in the TAG hydrothermal field, Mid-Atlantic ridge 26°N, 45°W. *J. Geophys. Res.* **98**, 9715–9730.

Rona, P.A., Fujioka, K., Ishihara, T., Chiba, H., Masuda-Nakaya, H., Omori, T., Kleinrock, M.C., Tivey, M.A., Watanabe, M., Lalou, C., 1998. An active low-temperature hydrothermal mound and a large inactive sulfide mound found in the TAG hydrothermal field, Mid-Atlantic Ridge 26N, 45W. *EOS Trans. AGU* **79**, F920.

Sachsenberg, S., Klenke, T., Krumbein, W.E., Schellhuber, H.J., Zeeck, E., 1993. Direct graphite furnace atomic absorption spectrometric determination of metals in sea water: application of palladium modifiers and a fractal approach to their analytical support. *Anal. Chim. Acta* **279**, 241–251.

Sansone, F.J., Mottl, M.J., Olsen, E.J., Wheat, C.G., Lilley, M.D., 1998. CO_2-depleted fluids from mid-ocean ridge-flank hydrothermal springs. *Geochim. Cosmochim. Acta* **62**, 2247–2252.

Schink, B., 1997. Energetics of syntropic cooperation in methanogenic degradation. *Microbiol. Mol. Biol. Rev.* **61**, 262–280.

Schippers, A., Jørgensen, B.B., 2001. Oxidation of pyrite and iron sulfide by manganese dioxide in marine sediments. *Geochim. Cosmochim. Acta* **65**, 915–922.

Schippers, A., Jørgensen, B.B., 2002. Biogeochemistry of pyrite and iron sulfide oxidation in marine sediments. *Geochim. Cosmochim. Acta* **66**, 85–92.

Schippers, A., Neretin, L.N., Kallmeyer, J., Ferdelman, T.G., Cragg, B.A., John Parkes, R., Jorgensen, B.B., 2005. Prokaryotic cells of the deep sub-seafloor biosphere identified as living bacteria. *Nature* **433**, 861–864.

Schrenk, M.O., Edwards, K.J., Goodman, R.M., Hamers, R.J., Banfield, J.F., 1998. Distribution of *Thiobacillus ferrooxidans* and *Leptospirillum ferrooxidans*; implications for generation of acid mine drainage. *Science* **279**, 1519–1522.

Schultz, A., Dickson, P., Elderfield, H., 1996. Temporal variations in diffuse hydrothermal flow at TAG. *Geophys. Res. Lett.* **23**, 3471–3474.

Scott, M.R., Scott, R.B., Morse, J.W., Betzer, P.R., Butler, L.W., Rona, P.A., 1978. Metal-enriched sediments from the TAG hydrothermal field. *Nature* **276**, 811–813.

Severmann, S., Mills, R.A., Palmer, M.R., Fallick, A.E., 2004. The origin of clay minerals in active and relict hydrothermal deposits. *Geochim. Cosmochim. Acta* **68**, 73–88.

Shaw, T.J., Gieskes, J., Jahnke, R.A., 1990. Early diagenesis in differing depositional environments: the response of transition metals in pore water. *Geochim. Cosmochim. Acta* **54**, 1233–1246.

Simoneit, B.R.T., Mazurek, M.A., Brenner, S., Crisp, P.T., Kaplan, I.R., 1979. Organic geochemistry of recent sediments from Guaymas Basin, Gulf of California. *Deep-Sea Res.* **26**, 879–891.

Singer, P.C., Stumm, W., 1970. Acid mine drainage: the rate determining step. *Science* **167**, 1121–1123.

Sobolev, D., Roden, E.E., 2004. Characterization of neutrophilic, chemolithoautotrophic Fe(II)-oxidizing β-proteobacterium from freshwater wetland sediments. *Geomicrobiol. J.* **21**, 1–10.

Sørensen, J., Christensen, D., Jørgensen, B.B., 1981. Volatile fatty acids and hydrogen as substrates for sulfate-reducing bacteria in anaerobic marine sediments. *Appl. Environ. Microbiol.* **42**, 5–11.

Sørensen, J., Jørgensen, B.B., 1987. Early diagenesis in sediments from Danish coastal waters: microbial activity and Mn-Fe-S geochemistry. *Geochim. Cosmochim. Acta* **51**, 1583–1590.

Telling, J., 2001. The Geomicrobiology of Deep-Sea Sediments on the Mid-Atlantic Ridge. Ph.D., University of Bristol.

Thamdrup, B., Canfield, D.E., 1996. Pathways of carbon oxidation in continental margin sediments off central Chile. *Limnol. Oceanogr.* **41**, 1629–1650.

Thamdrup, B., Fossing, H., Jørgensen, B.B., 1994. Manganese, iron, and sulfur cycling in a coastal marine sediment, Aarhus Bay, Denmark. *Geochim. Cosmochim. Acta* **58**, 5115–5129.

Thompson, G., Mottl, M.J., Rona, P.A., 1985. Morphology, mineralogy and chemistry of hydrothermal deposits from the TAG area, 26° N Mid-Atlantic Ridge. *Chem. Geol.* **49**, 243–257.

Thomson, J., Colley, S., Higgs, N.C., Hydes, D.J., Wilson, T.R.S., Sørensen, J., 1987. Geochemical oxidation fronts in NE Atlantic distal turbidites and their effects in the sedimentary record. In: Weaver, P.P.E., Thomson, J. (Eds.), *Geology and Geochemistry of Abyssal Plains*. Geological Society Special Publication 31, pp. 167–177.

Thomson, J., Higgs, N.C., Colley, S., 1996. Diagenetic redistribution of redox-sensitive elements in northeast Atlantic glacial/interglacial transition sediments. *Earth Planet. Sci. Lett.* **139**, 365–377.

Thomson, J., Jarvis, I., Green, D.R.H., Green, D.A., Clayton, T., 1998. Mobility and immobility of redox-sensitive elements in deep-sea turbidites during shallow burial. *Geochim. Cosmochim. Acta* **62**, 643–656.

Tivey, M.K., Humphris, S.E., Thompson, G., Hannington, M.D., Rona, P.A., 1995. Deducing patterns of fluid flow and mixing within the TAG active hydrothermal mound using mineralogical and geochemical data. *J. Geophys. Res.* **100**, 12,427–12,555.

Ueshima, M., Tazaki, K., 2001. Possible role of microbial polysaccharides in Nontronite formation. *Clays Clay Miner.* **49**, 292–299.

Vargas, M., Kashefi, K., Blunt-Harris, E.L., Lovley, D.R., 1998. Microbiological evidence for Fe(III) reduction on early Earth. *Nature* **395**, 65–67.

Wellsbury, P., Herbert, R.A., Parkes, R.J., 1993. Incorporation of methyl-H-3 thymidine by obligate and facultative anaerobic bacteria when grown under defined culture conditions. *FEMS Micobiol. Ecol.* **12**, 87–95.

Wellsbury, P., Parkes, R.J., 1995. Acetate bioavailability and turnover in an estuarine sediment. *FEMS Micobiol. Ecol.* **17**, 85–94.

Wheat, C.G., Mottl, M.J., 2000. Composition of pore and spring waters from Baby Bare: global implications of geochemical fluxes from a ridge flank hydrothermal system. *Geochim. Cosmochim. Acta* **64**, 629–642.

White, S.N., Humphris, S.E., Kleinrock, M.C., 1998. New observations on the distribution of past and present hydrothermal activity in the TAG area of the Mid-Atlantic Ridge (26°08′ N). *Mar. Geophys. Res.* **20**, 41–56.

Wirsen, C.O., Brinkhoff, T., Küver, J., Muyzer, G., Molyneaux, S., Jannasch, H.W., 1998. Comparison of a new Thiomicrospira strain from the Mid-Atlantic Ridge with known hydrothermal vent isolates. *Appl. Environ. Microbiol.* **64**, 4057–4059.

Wirsen, C.O., Jannasch, H.W., Molineaux, S.J., 1993. Chemosynthetic microbial activity at Mid-Atlantic Ridge hydrothermal vent sites. *J. Geophys. Res.* **98**, 9693–9703.

Wirsen, C.O., Tuttle, J.H., Jannasch, H.W., 1986. Activity of sulfur-oxidising bacteria at the 21°N East Pacific Rise vent site. *Mar. Biol.* **92**, 449–456.

Wolery, T.J., 1992. EQ3/6: A software Package for Geochemical Modelling of Aqueous Systems: Package Overview and Installation Guide, Livermore National Laboratory, Technical Report UCRL-MA-110662-PT-I.

Zeebe, R.E., Wolf-Gladrow, D. 2001. *CO_2 in Seawater: Equilibrium, Kinetics, Isotopes*. Elsevier Oceanography Series 65.